(1)

SEC

AD-A214 705

JMENTATION PAGE

Form Approved
OMB No. 0704-0188

1a.	1b. RESTRICTIVE MARKINGS
2a.	3. DISTRIBUTION / AVAILABILITY OF REPORT Approved for public release; distribution unlimited.
2b. DECLASSIFICATION / DOWNGRADING SCHEDULE	
4. PERFORMING ORGANIZATION REPORT NUMBER(S)	5. MONITORING ORGANIZATION REPORT NUMBER(S) AFOSR TR. 89 - [redacted] 1669
6a. NAME OF PERFORMING ORGANIZATION New York University Department of Applied Science	6b. OFFICE SYMBOL (If applicable)
6c. ADDRESS (City, State, and ZIP Code) Westbury, NY 11590	7a. NAME OF MONITORING ORGANIZATION AFOSR
	7b. ADDRESS (City, State, and ZIP Code) BLDG 410 BAFB DC 20332-6448
8a. NAME OF FUNDING / SPONSORING ORGANIZATION AFOSR	8b. OFFICE SYMBOL (If applicable)
	9. PROCUREMENT INSTRUMENT IDENTIFICATION NUMBER AFOSR-76-2497
8c. ADDRESS (City, State, and ZIP Code) BLDG 410 BAFB DC 20332-6448	10. SOURCE OF FUNDING NUMBERS

PROGRAM ELEMENT NO.	PROJECT NO.	TASK NO	WORK UNIT ACCESSION NO.
61102F	2307	A2	

11. TITLE (Include Security Classification)

INVESTIGATION OF THE FLUCTUATION MECHANISM IN TURBULENT FLOW

12. PERSONAL AUTHOR(S)
Victor Zakkay/ Vincent Barra

13a. TYPE OF REPORT	13b. TIME COVERED	14. DATE OF REPORT (Year, Month, Day)	15. PAGE COUNT
Final	FROM _____ TO _____	November 1979	35

16. SUPPLEMENTARY NOTATION

17. COSATI CODES			18. SUBJECT TERMS (Continue on reverse if necessary and identify by block number)
FIELD	GROUP	SUB-GROUP	

19. ABSTRACT (Continue on reverse if necessary and identify by block number)

89 11 27 160

20. DISTRIBUTION / AVAILABILITY OF ABSTRACT	21. ABSTRACT SECURITY CLASSIFICATION
☒ UNCLASSIFIED/UNLIMITED ☐ SAME AS RPT ☐ DTIC USERS	unclassified

22a NAME OF RESPONSIBLE INDIVIDUAL	22b. TELEPHONE (Include Area Code)	22c. OFFICE SYMBOL

DD Form 1473, JUN 86 — Previous editions are obsolete. — SECURITY CLASSIFICATION OF THIS PAGE

DISCLAIMER NOTICE

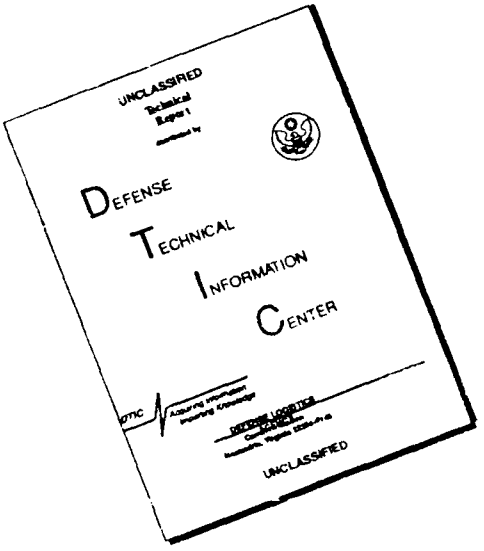

THIS DOCUMENT IS BEST QUALITY AVAILABLE. THE COPY FURNISHED TO DTIC CONTAINED A SIGNIFICANT NUMBER OF PAGES WHICH DO NOT REPRODUCE LEGIBLY.

1669

INVESTIGATION OF THE FLUCTUATION MECHANISM IN TURBULENT FLOW

Victor Zakkay
Vincent Barra

Final ~~ANNUAL~~ REPORT

AFOSR-76-2497

November 1979

NEW YORK UNIVERSITY
DEPARTMENT OF APPLIED SCIENCE
ANTONIO FERRI LABORATORIES
MERRICK AND STEWART AVENUES
WESTBURY, L.I.N.Y. 11590 NEW YORK

PROGRESS SUMMARY

A description of the technical work performed, and the results obtained during the fourth year of Grant No. AFOSR-76-2497 is contained for the most part in the two attached papers. One is a presentation made at the International Congress on Instrumentation in Aerospace Simulation Facilities held on September 24-26, 1979 in Monterey, California. It describes in some detail the level of sophistication that has been achieved thus far in terms of instrumentation and data analysis for our investigation. The second paper, presented at the AGARD Conference on Turbulent Boundary Layers held at The Hague on September 24-26, 1979, summarizes the major results and conclusions which have been deduced from our measurements. This paper includes our first results from measurements of the coherent structure in the lateral direction. In addition, the following events have also taken place during the past year:

- Publication in the April, 1979 issue of the AIAA Journal of our paper "The Nature of Boundary Layer Turbulence at High Subsonic Speed."
- Oral presentation of "Coherent Structure of Turbulence at a High Subsonic Speed," at the ASME Gas Turbine Conference in San Diego, California, March 12-15, 1979.
- Presentation of the paper (referred to above in connection with the ICIASF) describing our instrumentation at the meeting of the Supersonic Tunnel Association

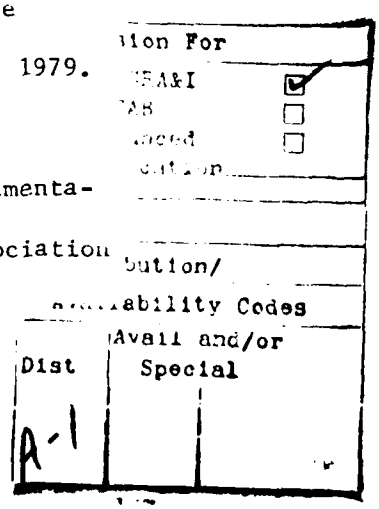

at Notre Dame University on September 13-14, 1979.

Since the preparation of these papers several important steps have been taken toward expanding our diagnostic capabilities and clarifying our understanding of the turbulent structure at high subsonic speeds. They are as follows:

- Construction, testing and utilization of 5 simple anemometer channels based on a circuit developed by Weidman and Browand at U.S.C. We have greatly improved the frequency response of the basic circuit by replacing the operational amplifier with one that has recently become available from Motorola. Five additional channels are about to be completed and our immediate goal is to have 15 of these units in operation. The advantage of the units lies in their relatively low-cost, the ease with which they can be set-up, and the improvement they allow in matching frequency response characteristics of different channels.
- At the present time, signal conditioning for the five working anemometer units have been provided for by the acquisition of a set of simple ac amplifiers. As more anemometer units become available, the additional signal conditioners required will have to be either purchased or constructed.
- With the five anamometer units operating five flush mounted hot-film shear sensors, recordings have been made

for a lateral grid which also includes five pressure transducers just upstream of the shear sensors and two streamwise velocity probes at a fixed height directly above two of the shear sensors (the original anemometer systems are still being used for the velocity probes). The obvious goal here would be to have five velocity probes in the grid but we are currently limited to 12 data channels on our Honeywell tape recorder. We are in the process of reactivating the Phillips tape recorder we were using in our early measurements which will make available five additional data channels. With the capacity to record up to 17 fluctuations in the flow it seems advisable to repeat the measurements with the previous streamwise - normal grid and use the additional channels to improve the resolution of the boundary layer velocity profile.

AGARD-CPP-271

AGARD

ADVISORY GROUP FOR AEROSPACE RESEARCH & DEVELOPMENT

7 RUE ANCELLE 92200 NEUILLY SUR SEINE FRANCE

AGARD CONFERENCE PREPRINT No. 271

Turbulent Boundary Layers – Experiments, Theory and Modelling

NORTH ATLANTIC TREATY ORGANIZATION

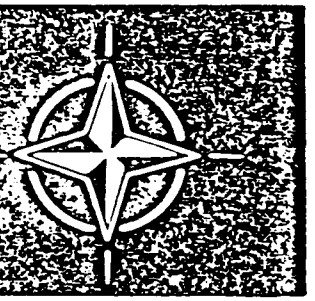

DISTRIBUTION AND AVAILABILITY
ON BACK COVER

V. Zakkay†, V. Barra††, and K. Hozumi†††
New York University
Department of Applied Science
26-36 Stuyvesant Street
New York, N.Y. 10003

Abstract

Results of simultaneous measurements of velocity, wall pressure, and wall-shear fluctuations in a turbulent boundary layer are presented. The measurements were performed in a range of velocities from 40-700 ft/sec, and a range of Re_θ from 10^4 to 10^5. The results are analyzed in an attempt to obtain a description of the coherent or quasi-ordered structure of the boundary layer turbulence. On a large scale, the boundary layer is dominated by vortical structures which extend to the viscid-inviscid region. The wall region is dominated by the so called "bursting" process. The relationship or interaction between the large scale outer structure and the turbulent "bursts" is still not clearly defined. The present experiments were particularly performed in order to understand how these processes develop and how their relationship changes with increasing Reynolds number. The results of this investigation at high speed, while confirming some of the previous results with regard to the mean period between coherent events, and their geometrical configuration, did not yet resolve the question as to whether at high subsonic speeds there is, besides the outer flow processes, a distinct inner region. With the limited instrumentation available it was not possible at the high subsonic speed to resolve any inner sublayer region, although it was found that the outer flow structures exert a strong influence on the wall. The experimental results at low subsonic speeds, on the other hand, did indeed identify an inner and outer region, and duplicated some of the results obtained at low subsonic speed by other investigations.

Introduction

The discovery, by means of visual observations (Refs. 1-7) of an organized structure in turbulent shear flows has led to a proliferation of new measurement and data analysis procedures for the investigation of the fluctuating properties of such flows (Ref. 8-19). Questions have been raised concerning the adequacy of measurements which utilize instrumentation and analyses not suited to the coherent, quasi-periodic nature of the flow structures. It has been found that the size of the transducers used in the measurements and the frequency response of the associated electronics is an important consideration in terms of the varied scales of the flow structures; and that single point measurements and conventional time averaged analyses cannot reveal much useful information about coherence or intermittency both of which are important aspects of the flow processes involved.

To overcome these problems, modern research efforts have turned to minituarized instrumentation and multiple measurements to obtain spatial resolution of the coherent flow structures, and to digitization of the measurements so as to allow various time series analyses to be performed on high speed computers. With respect to the latter, it has become increasingly popular to apply various conditional sampling procedures to the digitized fluctuations in order to isolate temporal sequences associated with the coherent structures. This type of analysis has revealed, among other things, that significant contributions to the long time average Reynolds stress occur during intervals when coherent structures are present in the flow, thus indicating that the modelling of turbulence and the development of drag and noise reduction mechanisms might benefit greatly from a better understanding of these structures.

Visual observations of turbulent boundary layer flows seeded with various tracers have indicated the presence of several different processes involving repetitive flow structures. The wall region ($y^+ = y\, u_\tau/\nu < 100$) is characterized by streamwise streaks of low speed fluid which lift up from the wall resulting in locally inflexional velocity profiles. The lift-up is followed by some sort of oscillatory motion and then a sudden breakup into small scale turbulence. The ejection of low speed fluid from the wall is accompanied by sweeps of high speed fluid from the outer regions toward the wall. This overall process has been referred to as a "burst" (Refs. 20-21). On a larger scale, the boundary layer is dominated by vortical structures which extend to the viscid-inviscid region (Refs. 6, 14, 16). The relationship or interaction between this large-scale outer structure (LSOS) and the turbulent "bursts" is still not clearly defined. In particular, how these processes and their relationship change with increasing Reynolds number has not been fully explored. On the basis of observations and measurements over a limited range of Reynolds numbers, it has become commonly accepted that the "bursting" process is strictly a sublayer phenomenon that scales with wall variables, while the large-scale outer structure is basically Reynolds number independent. A possible link between the two processes may exist in the fact that the frequency of occurrence of the turbulent "bursts" has been found to scale with outer flow variables and seems to be related to the period of passage of the outer structures (Refs. 22-23).

The primary goal of this investigation has been directed to study these phenomena at a high subsonic speed, and to specifically determine the possible role or influence of pressure fluctuations on the processes involved. Whereas most studies in this area tend to be at relatively low free stream velocities (typically, $U_\infty < 100$ ft/sec) and Reynolds numbers ($Re_\theta < 10^4$), the present results are for a turbulent boundary layer with $U_\infty = 675$ ft/sec and $Re_\theta = 108{,}000$. In addition, simultaneous measurements of three properties of the turbulent flow, namely, the streamwise velocity, the wall shear and the wall pressure

---

† Chairman, Department of Applied Science, and Director of the Antonio Ferri Laboratories, New York University.

†† Research Scientist, Antonio Ferri Laboratories, New York University.

were made. Preliminary results from measurements at U_∞ = 75 ft/sec led to the conclusion that it would be of some value to have comparitive measurements at lower velocities. Therefore measurements for boundary layers with U_∞ = 73 ft/sec and U_∞ = 32 ft/sec were also made, and are presented for comparison.

Experimental Facilities and Procedures

The New York University one foot diameter induction tunnel was used for this research. The facility has been described in detail in Refs. 19 and 24. The capability of varying the velocity from 30 to 700 ft/sec has since been added to the wind tunnel. In addition the wind tunnel was modified so as to allow the test section to be located at several distances from the inlet of the tunnel. This allowed the measurements to be made at various distances from the inlet depending on the boundary layer thickness required (at the lowest velocity, a boundary layer thickness of 3" was reached within 15 ft of the tunnel inlet).

The development of the data gathering system and the analysis programs has been a major part of the present research program (see Ref. 19). The system has been greatly improved by the acquisition of a PDP-11/34 mini-computer and a 14 channel tape recorder. The mini-computer system includes 64K bytes of memory, two terminals - one of which is an interaction CRT graphics terminal, floppy and cartridge disk mass storage, and most significantly, a 64 channel A/D converter with two programmable clocks. Programs have been developed on this system which are capable of performing the following analysis on a production run basis:

1) Long-time average auto and cross correlations.

2) Conditional sampling using the variable interval time average (VITA) variance (see Kaplan and Laufer (Ref. 25) or Blackwelder and Kaplan (Ref. 8)).

3) Pattern recognition analysis to compensate for random phase "jitter" in conditional samples (see Blackwelder (Ref. 26)).

4) Short-time, conditionally sampled auto and cross correlations (see Brown and Thomas (Ref. 14)).

These analyses can be applied directly to the original digitized data or to the data after it has been filtered using the Fast Fourier Transform to include only components within a chosen bandpass. In this way it should be possible to determine the importance or influence of different frequency ranges on particular results. From the use of the different analyses it should also be possible to determine if different approaches to conditional sampling produce comparable results when applied to the same data.

Test Conditions

In Ref. 19 experimental results were presented for U_∞ = 675 ft/sec. Since that time the measurements have been repeated for two new sensor arrays and more extensive analyses have been performed. In addition, extensive mean and fluctuating flow measurements at $U_\infty \approx$ 75 ft/sec and $U_\infty \approx$ 30 ft/sec have also been made. The mean flow properties of the boundary layer at several stations along the tunnel for these three flow conditions are summarized in Table I. Simultaneous measurements of the fluctuations have been made primarily with the sensor array shown in Fig. 1 and more recently with that shown in Fig. 2. In the latter, six wall-shear measurements are oriented so as to yield information about the turbulent structure in the lateral directions. The present results are for data from the following test conditions:

- U_∞ = 675 ft/sec, X/D = 31, Both arrays (i.e., Figs. 1 and 2)
- U_∞ = 73 ft/sec, X/D = 15.5, Fig. 1 array only
- U_∞ = 75 ft/sec, X/D = 20.5, Fig. 2 array only
- U_∞ = 32.6 ft/sec, X/D = 20.5, Both arrays

The aim of these tests is to yield data over a wide range of Reynolds numbers (i.e., from approximately 5000 to 100,000) while maintaining the boundary layer thickness in the neighborhood of 3 to 4 inches. The friction velocity, an important parameter in terms of the wall layer, also takes on a wide range of values for these tests, that is, from 1.8 ft/sec to 18 ft/sec.

Discussion of Measurements

A. Velocity, Wall-Shear and Wall-Pressure (Fig. 1)

Spectral analyses of the measured fluctuations have shown basic agreement with previous measurements except in the case of the pressure fluctuations in the two low speed cases (U_∞ = 73 ft/sec and U_∞ = 32.6 ft/sec). As the result of many previous measurements it is to be expected that the rms level of the wall-pressure fluctuations will fall somewhere between 0.5% and 1% of the dynamic pressure, q_∞. In the case of U_∞ = 675 ft/sec a reasonable level of 0.008 q_∞ was measured. But at U_∞ = 73 ft/sec and 32.6 ft/sec the measured levels were equivalent to approximately 0.23 q_∞ and 0.65 q_∞, respectively. The explanation for this is that, for the low speed tests, the wall-pressure fluctuations due to the turbulent boundary layer become so weak that they drop below the noise "floor" of the measuring devices. The noise "floor" is made up primarily of tunnel noise, although other sources such as transducer vibration response and mis-allignment with the tunnel wall may also contribute to it.

Research performed by other investigators, determined that the level of tunnel noise could be lowered with extensive acoustic treatment of the sonic throat section of the tunnel (where the flow undergoes rapid acceleration) and by improving the suspension system of the tunnel. These modifications were not undertaken for several reasons. First, in the high subsonic regime where the primary interest lies, the wall-pressure fluctuations due to the turbulent boundary layer are found to be sufficiently above the noise "floor" to allow for accurate measurements. Secondly, in the low speed case the main interest is in looking

... much greater sensitivity than the ones that are presently being used.

Sections of the data are digitized for all three free stream velocities and for both of the measurement arrays shown in Figs. 1 and 2. Various combinations of the analyses listed previously are applied to the digitized data in an attempt to obtain results comparable to those found by other investigators and to compare certain properties of the quasi-ordered turbulent structure at the varied flow conditions. It is becoming more evident from continued use of the VITA variance analysis that one must be carefull when looking at the mean period between events detected with this scheme. The number of times that the analysis will indicate the occurrence of an event in a fluctuating quantity used as a trigger will depend strongly on the threshold level applied to the VITA variance of that quantity. The results indicate that for all three free-stream velocities a threshold level equal to approximately one-half the long time rms of the fluctuating quantity in most cases yields a mean period between events given by $TU_\infty/\delta \approx 5$, although this will vary depending on the measurement used as the trigger. However, this period does not seem to be any more significant than any other that is obtained from this analysis with a different threshold. Some other criteria would have to be used to determine the threshold which has physical meaning in terms of a specific type of organized structure.

Although care must be taken when interpreting the mean period between events obtained in this way, an ensemble average of a set of events detected using the VITA variance can be helpful in depicting average or typical characteristics of coherent structures in the flow. Such a set of ensemble averages of the velocity and wall-shear fluctuations are shown in Figs. 3-5 for the three flow conditions and for the array shown in Fig. 1. They were obtained by applying the VITA variance analysis to the velocity fluctuations at y = .075"(O) to obtain a set of times where the fluctuations at this point indicate the occurrence of flow processes with certain repetitive characteristics. An ensemble average is then taken of 512 data points centered about these times for each of the six velocity and one wall-shear measurement. It can be seen from Fig. 3, that for U_∞ = 675 ft/sec there is a definite correlation across all seven measurements; that is, the average structure that the analysis triggers on encompasses, or at least has a strong influence on, all seven measurements. That is not the case for the two low speed flows. Figures 4 and 5 show that, for the trigger at y = .075"(O) (i.e., in the wall region), the average structure extends or correlates only over the three or four measurements nearest the wall. The fact that this correlation seems to extend almost twice as far from the wall (i.e., to y = .275"(K)) for U_∞ = 32.6 ft/sec (Fig. 5) than for U_∞ = 73 ft/sec (Fig. 4) may be an indication that this inner region shrinks toward the wall with increasing flow velocity, or alternatively, that it scales with wall variables.

To see whether a similar coherence exists in the outer measurements for the low speed flows, the analysis was repeated using the measurement at y = .375"(J) as a trigger. The results, shown in Figs. 6 and 7, indicate that there is a correlated structure in the outer region which does not seem to extend further down than y = .275"(K) from the wall. How far up in the boundary layer this coherence extends cannot be deduced from the present measurements.

An attempt has been made to determine if the loss of coherence with distance is due to noise that enters into the ensemble averages because of random variations in the phase between the events at the trigger and that at the measurement being averaged (see Blackwelder (Ref. 26)). A pattern recognition analysis was applied to adjust the phase, with respect to the trigger at y = .075"(O), of each event in the ensemble averages. The results shown in Figs. 8 and 9 are to be compared to Figs. 4 and 5, respectively. Since each event in the ensemble averages has been shifted to zero time delay, the averaged events are centered about t = 0 in all cases. The actual phase relationship of each average to the trigger at y = .075"(O) is given by the average shift of all the events in the ensemble. This is shown for each measurement position on both figures. It can be seen that for U_∞ = 73 ft/sec (Fifs. 4 and 8) this phase correction procedure has little effect in improving the ensemble averages, thus indicating that the loss of coherence in the outer measurements is not due to random phase "jitter" but rather to the fact that the flow structures in the wall region do not, on the average, extend beyond y $\approx$ .075" - .175" ($y^+ \approx$ 112-261). On the other hand, the phase correction procedure does result in a definite improvement in some of the averages for U_∞ = 32.6 ft/sec (Figs. 5 and 8). This is particularly evident at y = .175"(L) and to a significantly lesser degree at y = .275"(K). Thus, after correction for phase "jitter" it becomes more clear that as the velocity is lowered the coherence of the inner structure extends further from the wall (i.e., to y $\approx$ .175" - .275" for U_∞ = 32.6 ft/sec) or perhaps that the inner region scales with wall variables ($y^+ \approx$ 100-252). The results of Fig. 3 for U_∞ = 675 ft/sec are not inconsistent with this conclusion since all the measurements except the wall-shear are outside the wall region and the high degree of correlation of this measurement with the outer region may be only in terms of the low frequency components associated with the outer structure. This will be discussed further in the following paragraphs.

The ensemble averaged velocity and wall-shear fluctuations shown in Fig. 3 for U_∞ = 675 ft/sec can be plotted to yield a sequence of fluctuating velocity profiles which are presented in Figure 10. The instantaneous total velocity profiles corresponding to this sequence are shown in Fig. 11. These profiles show a great many similarities to those which have been measured in the wall region of low speed boundary layer flows, in particular, to those obtained by Blackwelder and Kaplan (Ref. 8). Attempts to depict the profiles in the low speed cases is hindered by the limited number of measurements in a given region, but indications are that the flow structures in both the inner and outer regions show the same type of coherence. (A similar conclusion was reached by Chen and Blackwelder (Ref. 16) from measurements of velocity and temperature in a boundary layer over a slightly heated wall). It is not possible to say whether these similarities are a result of the fact that the wall region "bursts" possess the same type of time signatures in terms of the streamwise velocity as the large scale outer structure or that they are a consequence of the detection scheme being used, that is to say, the detection scheme triggers on some "typical" structure which exists in both regions.

On the assumption that the former is the case, the available data will be analyzed further to determine what relationship exists between measurements in the inner and outer regions. From this, some insight may be gained into a possible interaction mechanism between the wall region "bursts" and the large

ranges it may be possible to isolate the components associated with the "bursting" process and to determine what relationship exists between these and the large scale flow structures. The success of such an analysis will depend strongly on the ability to accurately resolve the very small scales associated with turbulent "bursts". In this regard, a commercially available pressure transducer having a diameter of 0.010" will be tested and its output compared to that from the transducers now being used (d = 0.040").

Some preliminary results have been obtained concerning the behavior of the wall pressure fluctuations from the measurements and data discussed in Ref. 19 for U_∞ = 675 ft/sec. The measurement grid was similar to that shown in Fig. 1 except that fewer sensors were available at that time and the streamwise velocity was measured at slightly different positions. Figure 12 shows the result of taking the ensemble average of 60 events detected over an interval of TU_∞/δ^* = 2000 using the velocity fluctuations at y/δ^* = 0.088 as the trigger. The velocity and shear fluctuations are basically the same as those in Fig. 3 since the trigger is at approximately the same position in both cases. From Fig. 12 the wall pressure fluctuations can be seen to be characterized by a well defined period of overpressure during the passage of the flow structures in the outer region. An examination of the wall pressure fluctuations during individual events consistently shows the superposition of large amplitude high frequency components on the more slowly varying period of overpressure. The fact that these high frequency components do not appear on the average would indicate that they are either a random phenomenon or that they occur at a random phase with respect to the process which triggers the detection scheme. It should be possible to determine which is the case by filtering the pressure fluctuations to obtain some representation of the high frequency components and then applying a detection scheme to see if coherence also exists in this aspect of the data. A dominant phase relationship between the low and high frequency components of the fluctuations could also be determined by cross-correlating the two.

B. Wall-Shear Measurements in the Lateral Direction (Fig. 2)

Measurements with the wall-shear array shown in Fig. 2 have been analyzed for U_∞ = 675, 75, and 32.6 ft/sec. Figures 13-15 show the results of taking ensemble averages at each position using the measurement at C as the trigger for detecting the occurrence of events. It can be seen that except for the high speed case (Fig. 13) there is no discernible correlation in the lateral direction, whereas a definite correlation exists for the measurement (F) oriented directly downstream of the trigger position. This is to be expected since previous measurements as well as visual observations have indicated that both the wall region "bursts" and the large scale outer structures maintain a high degree of coherence for large distances in the streamwise direction. The extent and spread of these structures in the lateral direction is much more limited. In the case of the wall region processes, for example, the separation between the streamwise streaks is estimated to be on the order of $Z^+ \approx 100$, while each individual streak is confined to a fraction of this distance.

It is not clear from the results of Figs. 13-15 whether the detection scheme we are using triggers on the wall region structures or on the response of the wall shear to the passage of the large scale outer structures. It can be seen from the non-dimensional distances in Fig. 2 that, at least in the case of U_∞ = 32.6 ft/sec, the size and separation of the wall shear sensors should be adequate for discerning some aspects of the wall region processes. However, several factors would seem to indicate that the typical wall shear response seen in the measurements at C and F in Figs. 13-15 is a result of the large scale outer structure. First, the typical response histories in the low speed cases (Figs. 14 and 15) consistently show that what appears to be an overshoot or superimposed high frequency component at the top of the rapid change in the wall shear. A similar phenomenon was observed by Brown and Thomas (Ref. 14) in their wall shear measurements and led them to speculate that the superimposed high frequency component was a manifestation of the "bursting" process. The high frequency component was seen to occur at a well determined phase with respect to the low frequency component attributable to the large scale outer structure, specifically, it occurred near positive maxima of the fluctuating shear. A similar conclusion concerning the present results would seem to be supported by the fact that this effect appears to be more pronounced in Fig. 15, i.e., U_∞ = 32.6 ft/sec (where better resolution is possible of the wall region processes) than in Fig. 14 for U_∞ = 75 ft/sec, and does not appear at all in Fig. 13 for U_∞ = 675 ft/sec where the instrumentation is not capable of resolving any processes on the scale of the wall region.

A second indication that the well defined time signatures in Figs. 13-15 are basically the response of the wall shear to the outer structure comes from the results of a phase correction analysis shown in Figs. 16 and 17 for U_∞ = 675 ft/sec, in Figs. 18 and 19 for U_∞ = 75 ft/sec and in Figs. 20 and 21 for U_∞ = 32.6 ft/sec. The set of events which are detected by using $\tau'(C)$ as a trigger are divided into two groups depending on the phase relationship between each event at C and any similar event found at B by the pattern recognition analysis referred to earlier. The search for a similar event was restricted to time delays approximately in the range $-5 < t'U_\infty/\delta^* < 5$. The ensemble averages obtained for the set of events where a match was found at a later time in $\tau'(B)$ (positive delay) are shown in Figs. 16, 18, and 20 and at an earlier time (negative delay) in Figs. 17, 19 and 21. The average time delay by which the events in each ensemble average were shifted is also indicated in these figures. The marked improvement, particularly for the two low speed cases, in the ensemble averages (compared to Figs. 13-15) shows that a coherence exists in the lateral direction which was previously obscured by random phase "jitter" and which extends across three or four of the measurements, i.e., $Z^+ \approx$ 500-5000. This could not be as a result of wall region processes which have been observed to be confined to lateral distances on the order of $Z^+ \approx 50$.

The fact that the events can be separated into two groups with opposite phase relationships across the lateral measurements is thought to be an indication of the "arrowhead" or "horseshow" type shape (see Fig. 2) that has been hypothesized for the large scale outer structure when looked at from above the wall of the boundary layer. It is clear that the phase relationship one would obtain among a set of lateral measurements would depend on which "leg" of the structure crosses the measurements. From the results of Figs. 16-21 it is possible to estimate the angles θ^+ and θ^- in Fig. 2 that each "leg" makes with the X-axis. Taking the average time delay between the measurements at C and F one obtains a streamwise convection velocity of U_c/U_∞ = 0.70 for U_∞ = 675 ft/sec, U_c/U_∞ = 0.69 for U_∞ = 75 ft/sec and U_c/U_∞ = 0.6[illegible] for U_∞ = 32.6 ft/sec. Using these [illegible]

θ^+ and θ^- are due to errors in the estimates, since by symmetry they should be equal. The results in the two low speed cases compare favorably with the angle of 22° estimated by Thomas (Ref. 15) from similar measurements at $U_\infty \sim 100$ ft/sec. The much smaller angle obtained in the high speed case could be an indication that the flow structure becomes more confined in the lateral direction as the free stream velocity is increased.

Conclusions

Measurements of the fluctuating properties of a turbulent boundary layer for a wide range of free stream conditions have been analyzed to obtain information concerning coherent or quasi-ordered structures in the flow. The primary interest of the investigation is for free stream velocities in the high subsonic regime (specifically, $U_\infty = 675$ ft/sec), although comparative measurements have been made at two lower velocities, i.e. $U_\infty \sim 75$ ft/sec and $U_\infty \sim 30$ ft/sec. The Reynolds number, Re_θ, ranges from 10^5 down to approximately 10^4, while the boundary layer thickness is maintained relatively constant at between 3 to 4 inches.

Recordings of the fluctuating streamwise velocity, wall-shear, and wall-pressure in the boundary layer are digitized to obtain simultaneous time histories of the fluctuations. These are analyzed on a minicomputer using various conditional sampling procedures to isolate temporal sequences associated with the coherent structures. From this the mean period between occurrences of the flow structures is estimated and ensemble averages found. These ensemble averages and cross-correlations between measurements at different positions during the occurrence of events are used to deduce information concerning the geometry of the flow structures.

Measurements for two arrays of sensors have been analyzed in this way. In one, wall-shear and wall-pressure sensors are aligned in the streamwise direction upstream of a rake of six streamwise velocity probes. In the other, wall-shear measurements are aligned so as to yield information about the flow structures in the lateral direction. Using a variable-interval time-average (VITA) variance analysis to detect the occurrence of events in the data, the mean period between events ($\bar{T}$) is found to be approximately given by $\bar{T}U_\infty/\delta_{.995} \sim 5$, although some variation is found depending on the measurement used as the trigger for detection. The number of events detected using this technique, however, is strongly dependent on the threshold chosen in the analysis. The estimate given here was obtained with thresholds in the neighborhood of one-half the overall rms of the fluctuations under consideration. But this choice seems rather arbitrary and the resulting mean period between events should be judged accordingly.

Irregardless of these questions about the number of events detected, a normalized ensemble average of all the events is useful in depicting certain characteristics of the flow structures. In the case of the streamwise velocity measurements normal to the wall for $U_\infty = 675$ ft/sec, it was found that the average structure correlates well over all the measurements including the wall-shear. This was not the case for the two low speed flows. If a measurement near the wall is used as a trigger the resulting ensemble averages display coherence only up to a certain distance from the wall (i.e., up to $y^+ \sim 100$-200). A similar coherence exists in the outer measurements when one of these is used as a trigger. In addition, the boundary between the inner and outer regions seems to be further from the wall for $U_\infty = 326$ ft/sec than for $U_\infty = 73$ ft/sec. This may be an indication that the inner region scales with wall variables.

The similarity of the coherence in the inner and outer regions as well as the similarity between the present measurements in the high speed case (which, except for the wall measurements, are in the outer region) and the results obtained by others in the wall region of low speed flows may be due to one of two reasons. Either the detection scheme being used triggers on some "typical" structure existing in various regions of the boundary layer, or the wall region "burst" process exhibits the same time signature in terms of the streamwise velocity as certain aspects of the large scale outer structure. It is not possible to determine from the present results which of these is actually the case.

Of particular interest in the high speed results is the fact that the coherence seen in the outer measurements extends to the wall. Both the wall-shear and the wall-pressure show a definite correlation to the passage of the outer structure. This is not the case, at least on the average, for the two low speed flows. By looking at individual events in the low speed measurements more carefully it should be possible to determine if there are events which exhibit some correlation between the inner and outer regions. To determine whether the strong correlation seen in the high speed measurements is due to the inability of the sensors to resolve the small scales associated with the wall region processes, a pressure transducer which is ¼ the size of those now being used will be tested. With regards to this question of the interaction between wall region processes and the large scale outer structure, an attempt will also be made to look at the measurements in various frequency ranges and to see what relationship exists between them.

Two important results were obtained from the wall-shear measurements which concentrated on the lateral aspects of these flow structure, or to be more precise, of their "footprint". From two measurements aligned in the streamwise direction, the average convection velocity of the flow structures was found to be in the range $U_c = 0.6 - 0.7\ U_\infty$. This result, combined with the phase relationship found between the same event as measured at two adjacent lateral position, was used to determine the angle that the sides of the flow structure makes with the streamwise direction. This angle was found to be approximately 20° for $U_\infty = 32.6$ ft/sec and 18° for $U_\infty = 75$ ft/sec. In the high speed case ($U_\infty = 675$ ft/sec) a much smaller angle of about 6° was estimated. This would seem to indicate that the flow structures tend to become more confined in the lateral direction as the flow velocity increases.

References

1. Kline, S.J., Reynolds, W.C., Schraub, F.A. and Runstadler, P.W., "The Structure of Turbulence," Journal of Fluid Mechanics, 30:741, 1967.

2. Corrino, E.R. and Bradley, R.S., "A Visual Investigation of the Wall Region in Turbulent Flow,"

3. Kim, H.T., Kline, S.J., and Reynolds, W.C., "The Production of Turbulence Near a Smooth Wall in a Turbulent Boundary Layer," Journal of Fluid Mechanics, 50:133, 1971.

4. Offen, G.R. and Kline, S.J., "Combined Dye Streak and Hydrogen bubble Visual Observations of a Turbulent Boundary Layer," Journal of Fluid Mechanics, 62:223, 1974.

5. Falco, R.E., "Some Coments on Turbulent Boundary Layer Structure Inferred from the Movements of a Passive Contaminant," AIAA Paper No. 74-99, 1974.

6. Falco, R.E., "Coherent Motions in the Outer Region of Turbulent Boundary Layer," Physics of Fluids, 20:S124, 1977.

7. Smith, C.A., "Visualization of Turbulent Boundary Layer Structure Using a Moving Hydrogen Bubble-Wire Probe," Proc. of the Workshop on Coherent Structure of Turbulent Boundary Layers, p. 48, 1978.

8. Blackwelder, R.F. and Kaplan, R.E., "The Intermittent Structure of the Wall Region of the Turbulent Boundary Layer," U. Southern California, A.E. Report No. 1-22, 1972.

9. Wallace, J.M., Eckelman, H., and Brodkey, R.A., "The Wall Region in Turbulent Shear Flow," Journal of Fluid Mechanics, 54-39, 1972.

10. Lu, S.S. and Willmarth, W.W., "Measurements of the Structure of the Reynolds Stress in a Turbulent Boundary Layer," Journal of Fluid Mechanics, 60:481, 1973.

11. Emmerling, R., "The Instantaneous Structure of the Wall Pressure Under a Turbulent Boundary Layer," Max-Planch-Institut fur Stromungschung, Rep. No. 9, 1973.

12. Dinkelacker, A., Hessel, M., Meier, G.E.A., and Schewe, G., "Investigation of Pressure Fluctuations Beneath a Turbulent Boundary Layer by Means of an Optical Method," Physics of Fluids, 20:S216, 1977.

13. Zilberman, M., Wyganski, I., and Kaplan, R., "Transitional Boundary Layer Spot in a Fully Turbulent Environment," Physics of Fluids, 20:S258, 1977.

14. Brown, G.L. and Thomas, A.S.W., "Large Structure in a Turbulent Boundary Layer," Physics of Fluids, 20:243, 1977.

15. Thomas, A.S.W., "Organized Structure in the Turbulent Boundary Layer," Lockheed-Georgia Report LG77ER0210, 1977.

16. Chen, C.P. and Blackwelder, R.F., "Large-scale Motion in a Turbulent Boundary Layer: A Study Using Temperature Contamination," Journal of Fluid Mechanics, 89:1, 1978.

17. Eckelmann, H., Wallace, J.M., and Brodkey, R.A., "Pattern Recognition, a Means for Detection of Coherent Structures in Bounded Turbulent Shear Flows," Proc. of the Dynamic Flow Conference, p. 161, 1978.

18. Wygnanski, I., "The Recognition of an Evoked Large-Scale Structure in Turbulent Shear Flows," Proc. of the Dynamic Flow Conference, p. 191, 1978.

19. Zakkay, V., Barra, V., and Wang, C.R., "The Nature of Boundary Layer Turbulence at a High Subsonic Speed," AIAA Journal, 17:356, 1978.

20. Offen, G.R. and Kline, S.J., "A Proposed Model of the Bursting Process in Turbulent Boundary Layers," Journal of Fluid Mechanics, 70:209, 1975.

21. Kline, S.J., "The Role of Visualization in the Study of the Structure of the Turbulent Boundary Layer," Proc. of the Workshop on Coherent Structure of Turbulent Boundary Layers, p. 1, 1978.

22. Rao, K.N., Narasismha, R., and Badri Narayanon, M.A., "The Bursting Phenomenon in a Turbulent Boundary Layer," Journal of Fluid Mechanics, 48:339, 1971.

23. Laufer, J. and Badri Narayanon, M.A., "Mean Period of the Production Mechanism in a Boundary Layer," Physics of Fluids, 14:182, 1971.

24. Zakkay, V., Barra, V., and Hozumi, K., "Investigation of the Fluctuation Mechanism in Turbulent Flow," Final Report prepared under Contract AFOSR-76,2497, December 1978.

25. Kaplan, R.E. and Laufer, J., "The Intermittently Turbulent Region of the Boundary Layer," 12th Proc. Int. Congr. Mech., p. 236, 1969.

26. Blackwelder, R.F., "On the Role of Phase Information in Conditional Sampling," Phys. Fluids, 20:S232, 1977.

X/D	15.5	20.5	9.	15,5	31.	31.
M_∞	0.0263	0.0296	0.063	0.067	0.072	.64
U_∞ (ft/sec)	29.6	32.6	69.0	73.0	79.0	675
q_∞ (psi)	0.0068	0.0086	0.039	0.046	0.054	2.9
δ (in)	2.7	3.5	2.15	3.0	$\approx$ 5.5	4.0
δ^* (in)	0.39	0.497	0.265	0.37	$\approx$ 0.8	0.564
θ (in)	0.31	0.387	0.206	0.29	$\approx$ 0.6	0.384
Re_θ	4.62×10^3	6.56×10^3	8.45×10^3	1.25×10^4	2.82×10^4	1.08×10^5
ν/u_τ(in)	1.66×10^{-3}	1.09×10^{-3}	$.69 \times 10^{-3}$	$.67 \times 10^{-3}$	$.68 \times 10^{-3}$	1.32×10^{-4}
ν/u_τ^2 (μsec)	120	51.6	24.0	22.5	23.0	0.62
$(u'/u)_\infty$	0.005	-	-	0.005	0.021	0.008

TABLE I

Mean Flow Parameters at Several Stations for Three Test Conditions

U_∞ (ft/sec)		675		73		32.6	
	y	y/δ^*	y^+	y/δ^*	y^+	y/δ^*	y^+
I	.475"	.85	3600	1.28	710	.95	436
J	.375"	.67	2840	1.01	560	.75	344
K	.275"	.49	2083	.74	410	.55	252
L	.175"	.313	1325	.473	261	.350	160
O	.075"	.134	568	.203	112	.150	69
M	.025"	.045	189	.068	37	.050	23

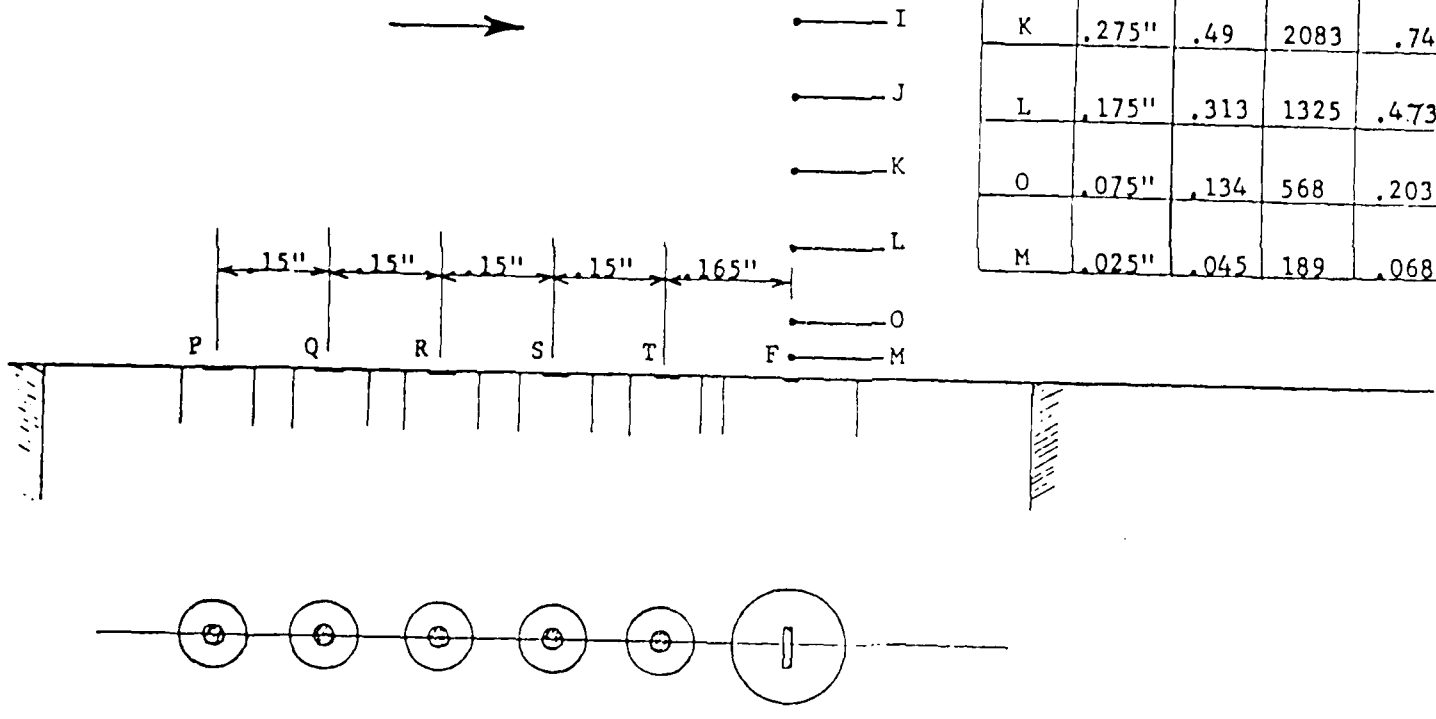

Fig.1 Sketch of instrumentation lay-out including table of non-dimensional distances from wall

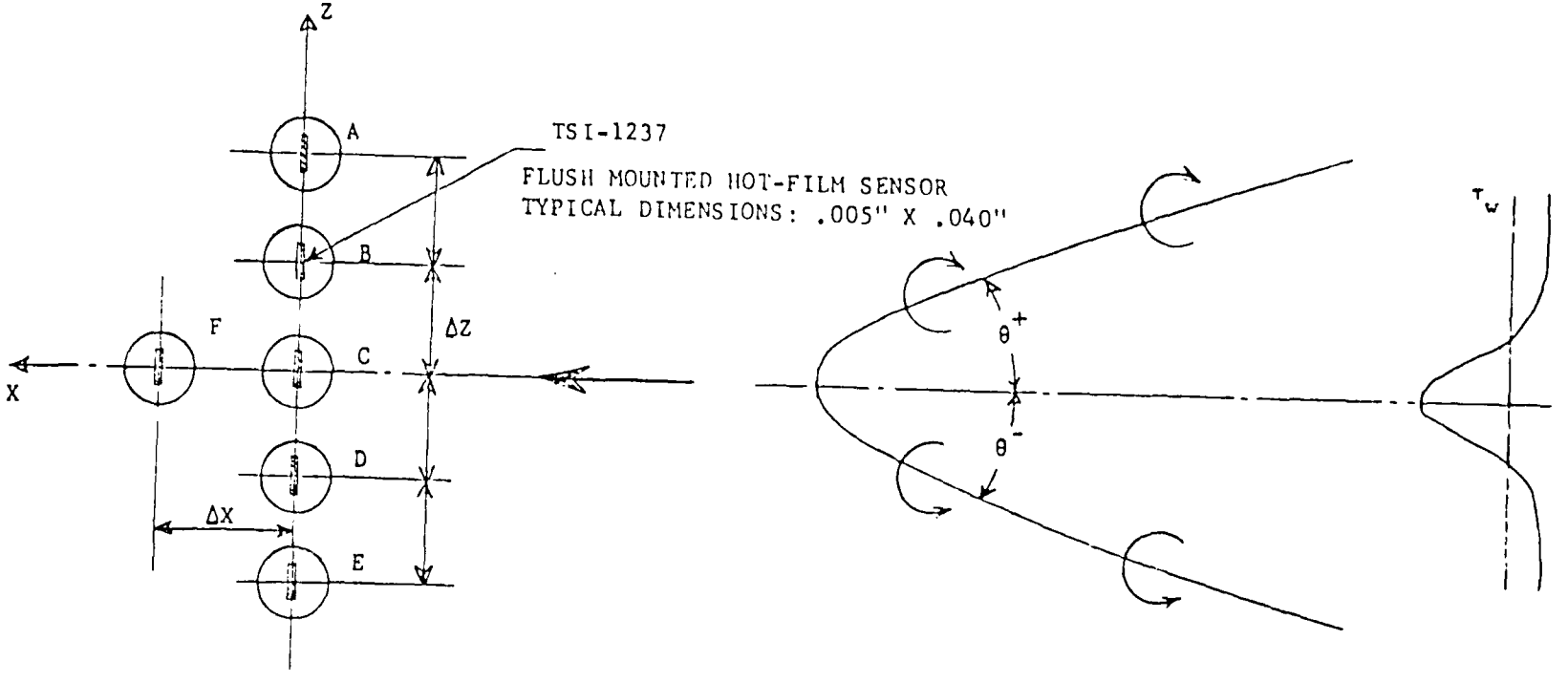

U_∞ (ft/sec)		675		75		32.6	
ΔX	ΔZ	ΔX^+	ΔZ^+	ΔX^+	ΔZ^+	ΔX^+	ΔZ^+
0.2"	0.157"	1540	1208	299	234	182	143

(Proposed plan view of large-scale outer structure from Thomas, Ref. 15)

Fig.2 Sketch of lateral array of flush-mounted hot-film sensors

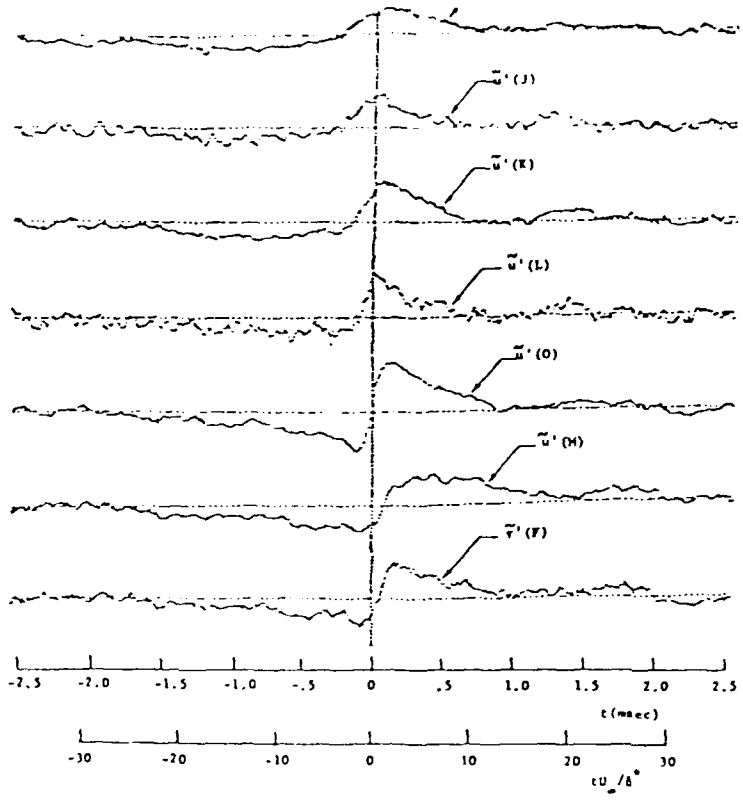

Fig.3 Ensemble averaged velocity and wall-shear fluctuations U_∞ = 675 ft/sec, trigger: u'(O)

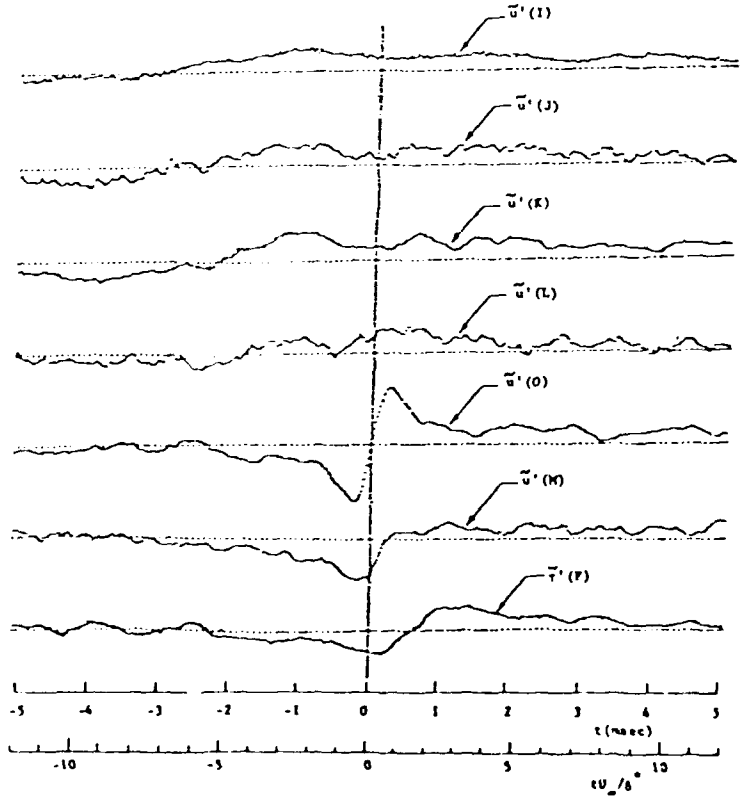

Fig.4 Ensemble averaged velocity and wall-shear fluctuations U_∞ = 73 ft/sec, trigger: u'(O)

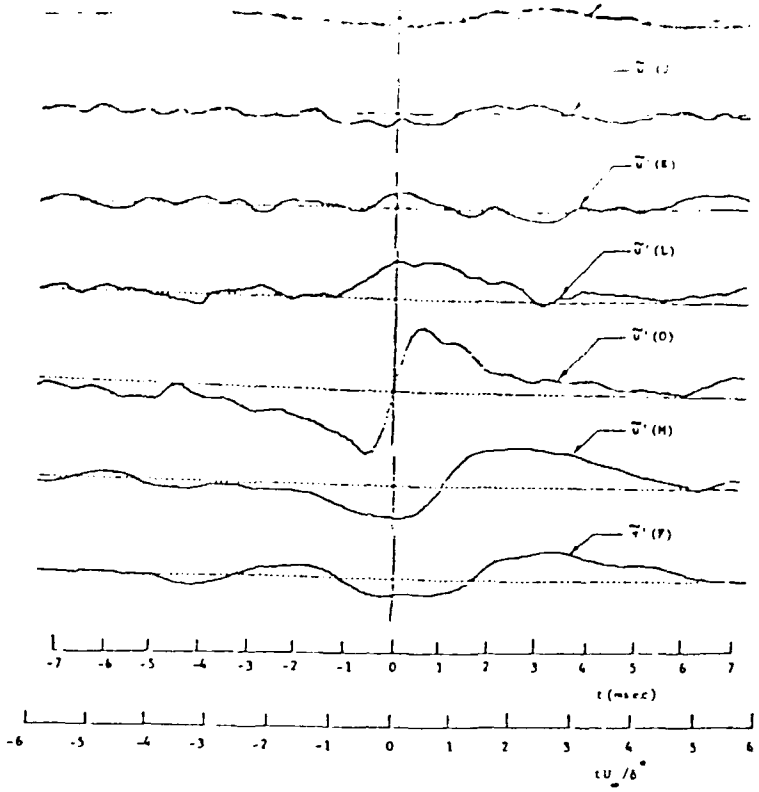

Fig.5 Ensemble averaged velocity and wall-shear fluctuations U_∞ = 32.6 ft/sec, trigger: u'(O)

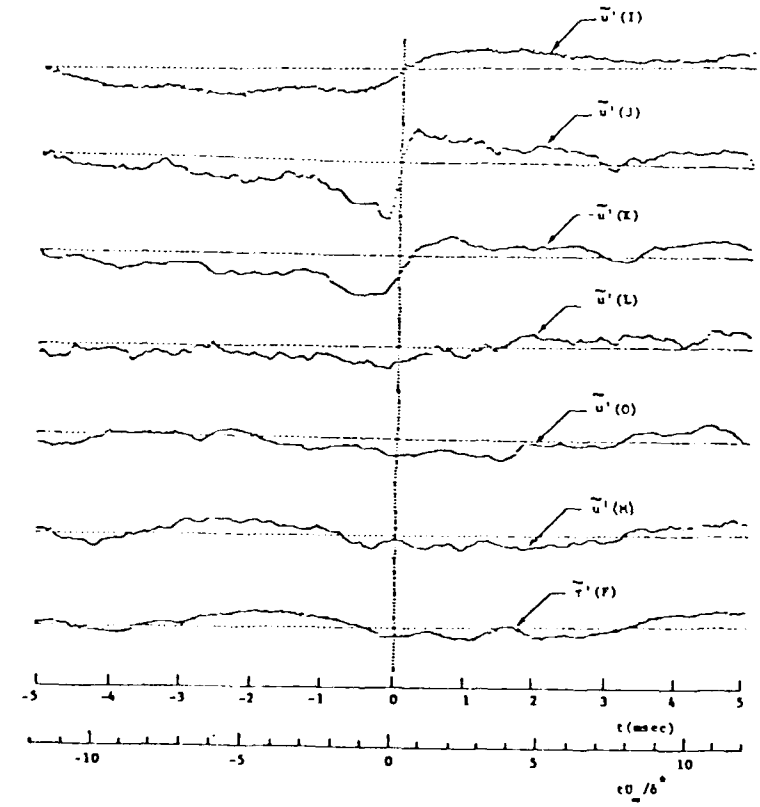

Fig.6 Ensemble averaged velocity and wall-shear fluctuations U_∞ = 73 ft/sec, trigger: u'(J)

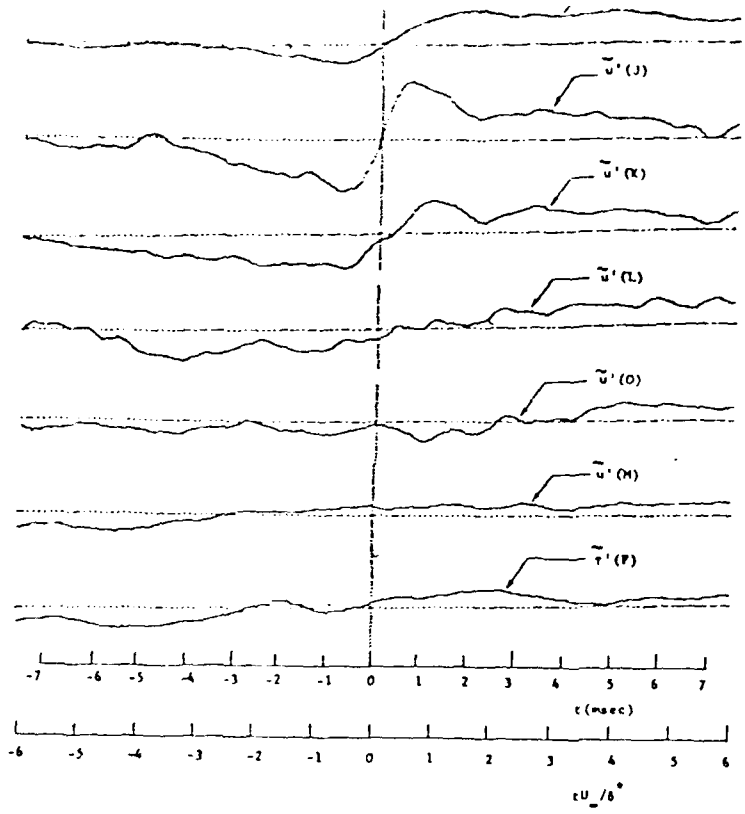

Fig.7 Ensemble averaged velocity and wall-shear fluctuations U_∞ = 32.6 ft/sec, trigger: u'(J)

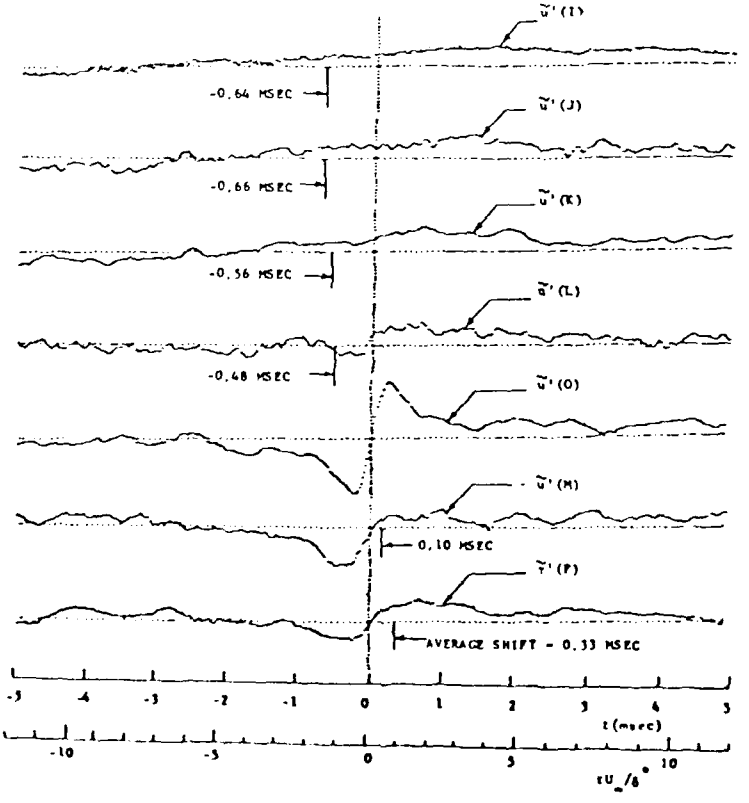

Fig.8 Ensemble averaged velocity and wall shear fluctuations after correction

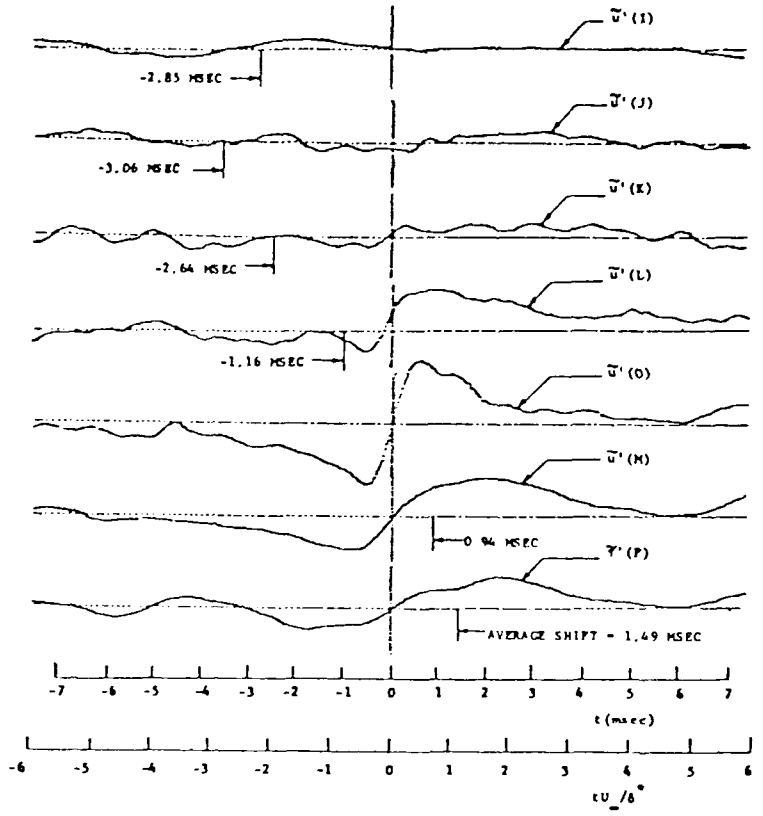

Fig.9 Ensemble averaged velocity and wall-shear fluctuations after correction for phase "jitter" – U_∞ = 32.6 ft/sec, trigger: u'(O)

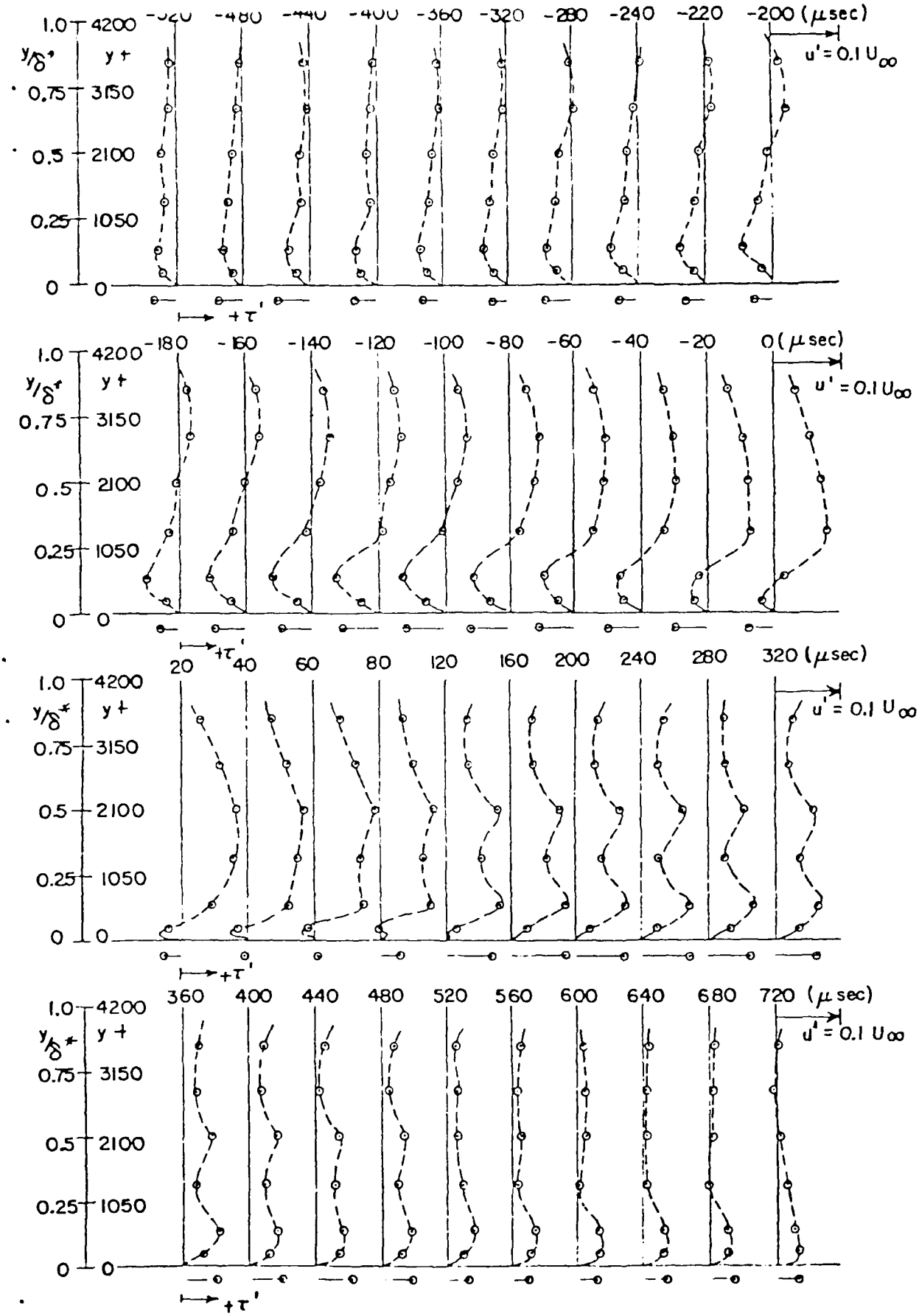

Fig 10 Sequence of velocity fluctuation profiles and fluctuating shear obtained

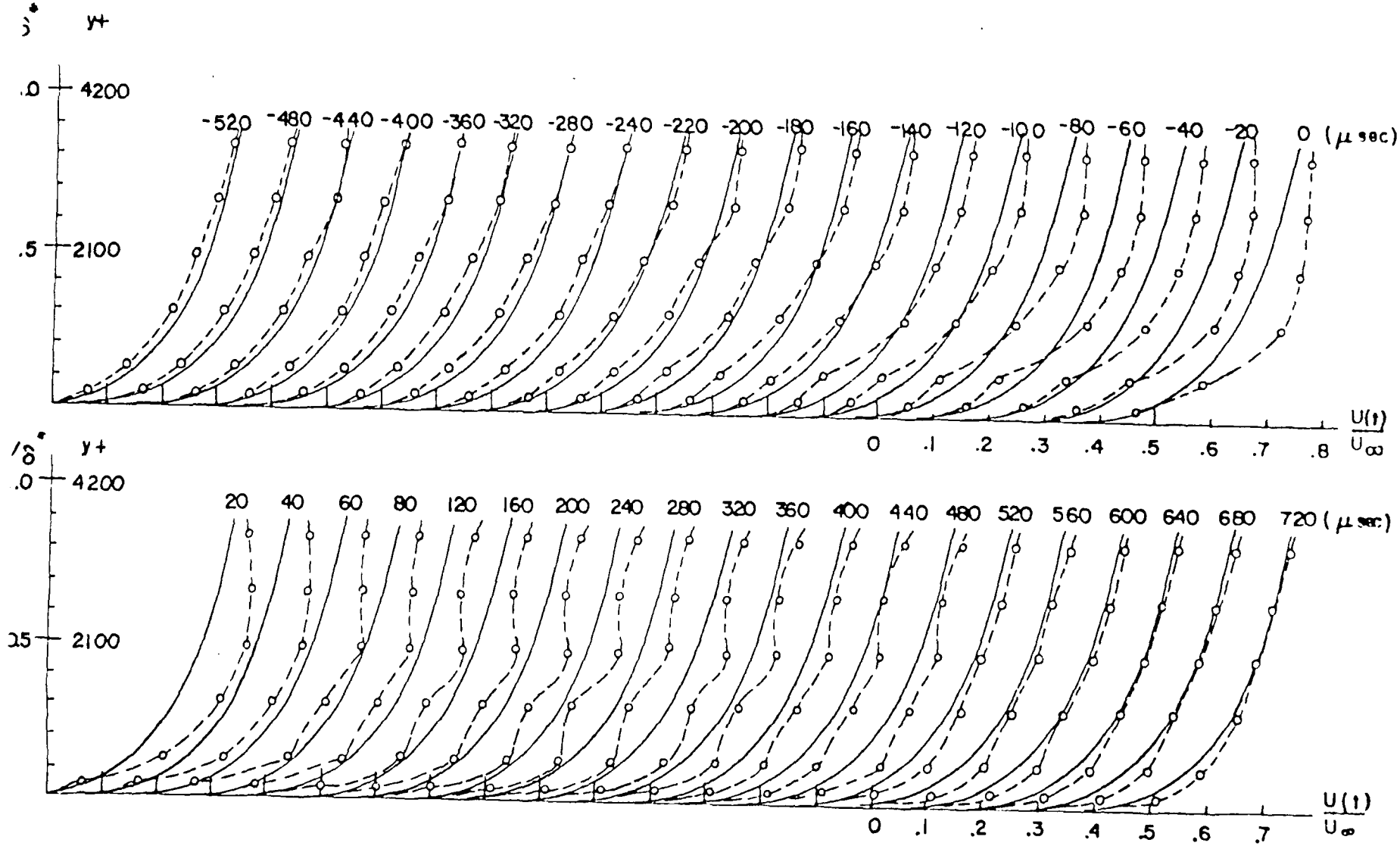

Fig.11 Sequence of total velocity profiles obtained from the ensemble averages in Figure 3 (U_∞ = 675 ft/sec)

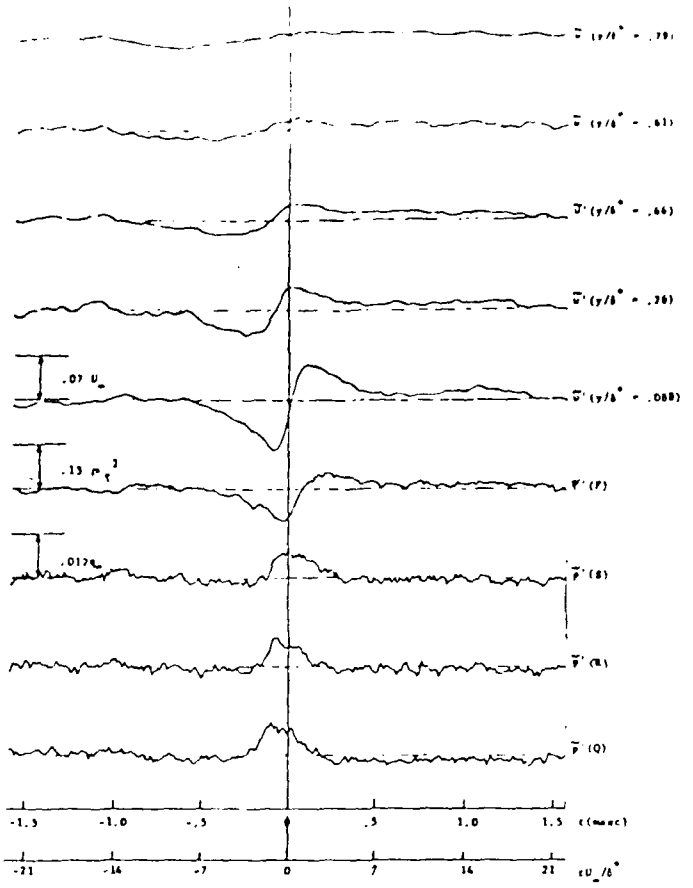

Fig.12 Ensemble averaged velocity shear and pressure fluctuations (from data of Reference 19)
U_∞ = 675 ft/sec, trigger: $u'(y/\delta^* = .088)$

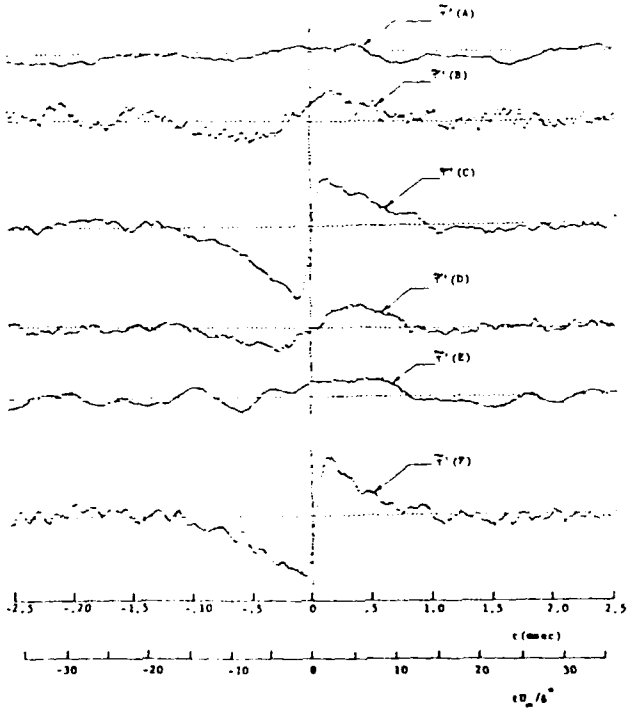

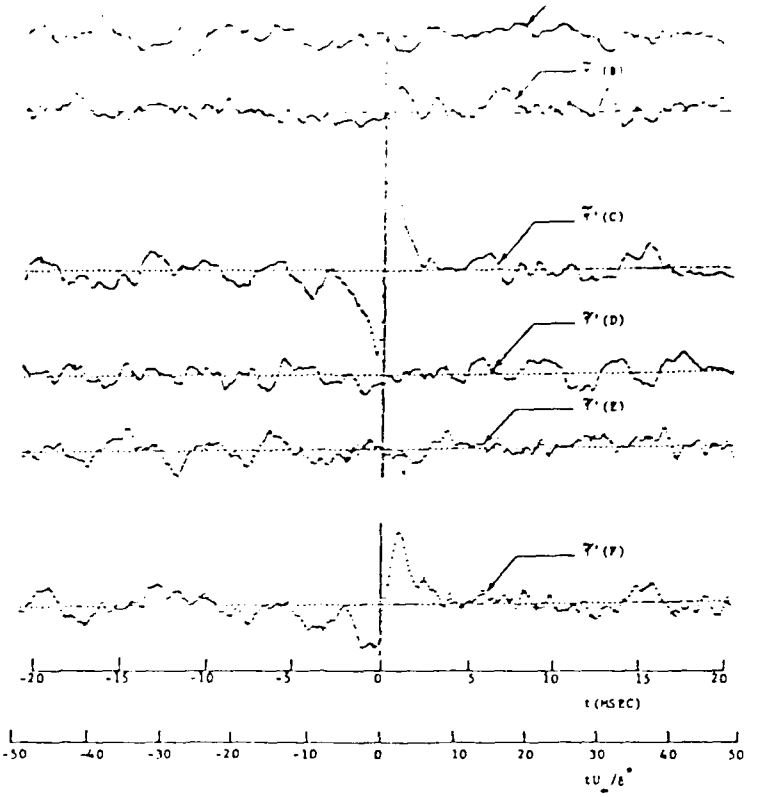

Fig.14 Ensemble averaged wall shear fluctuations for array in Figure 2
U_∞ = 75 ft/sec, trigger: $\tau'(C)$

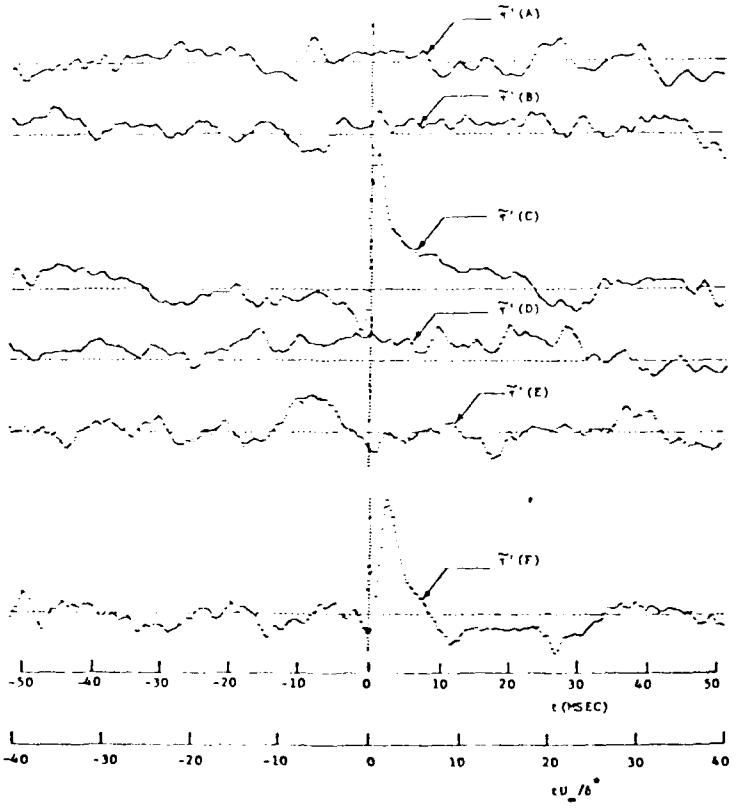

Fig.15 Ensemble averaged wall shear fluctuations for array in Figure 2

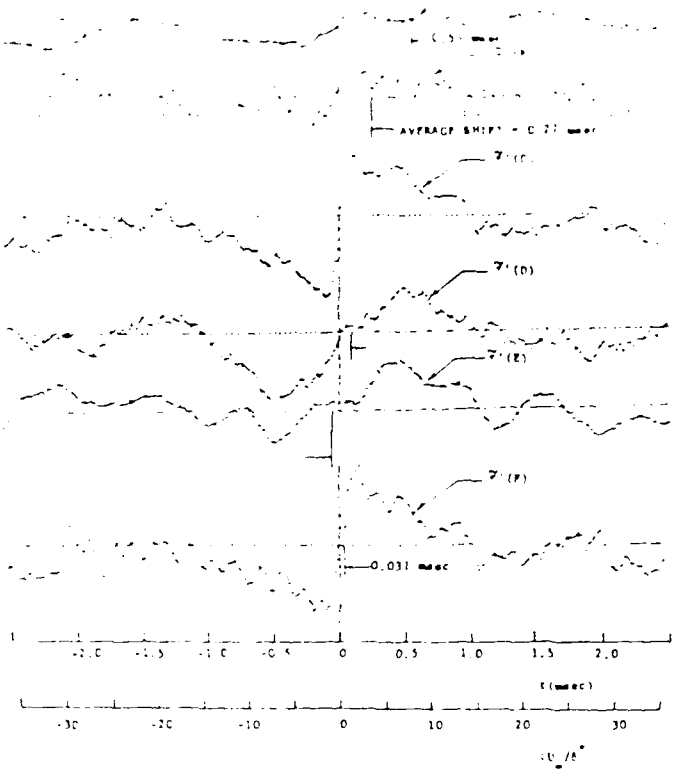

Fig 16 Ensemble averaged wall shear fluctuations for the array of Figure 2 after correction for phase "jitter" (only events with positive shifts between $\tau'(C)$ and $\tau'(B)$)
U_∞ = 675 ft/sec, trigger: $\tau'(C)$

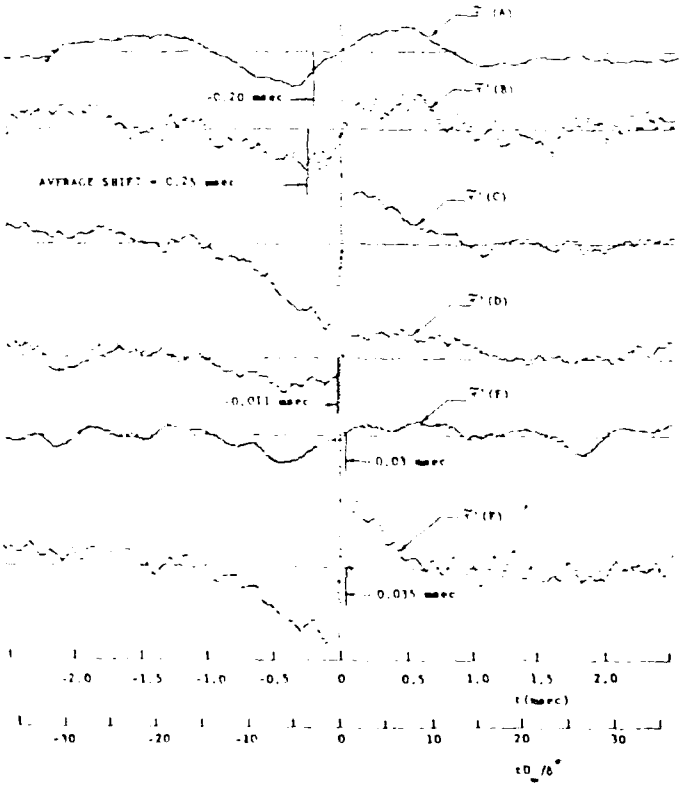

Fig 17 Ensemble averaged wall shear flucutations for the array of Figure 2 after correction for

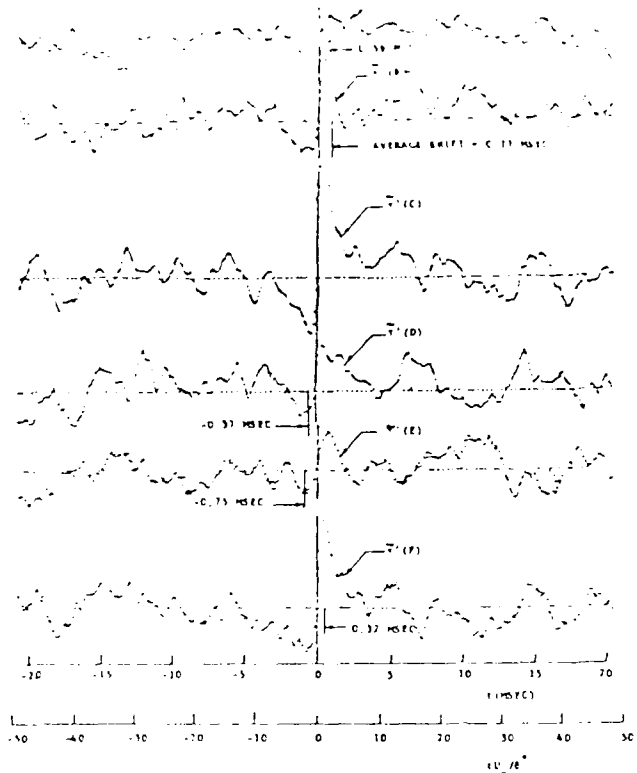

Fig 18 Ensemble averaged wall shear fluctuations for the array of Figure 2 after correction for phase "jitter" (only events with positive shifts between $\tau'(C)$ and $\tau'(B)$)
U_∞ = 75 ft/sec, trigger: $\tau'(C)$

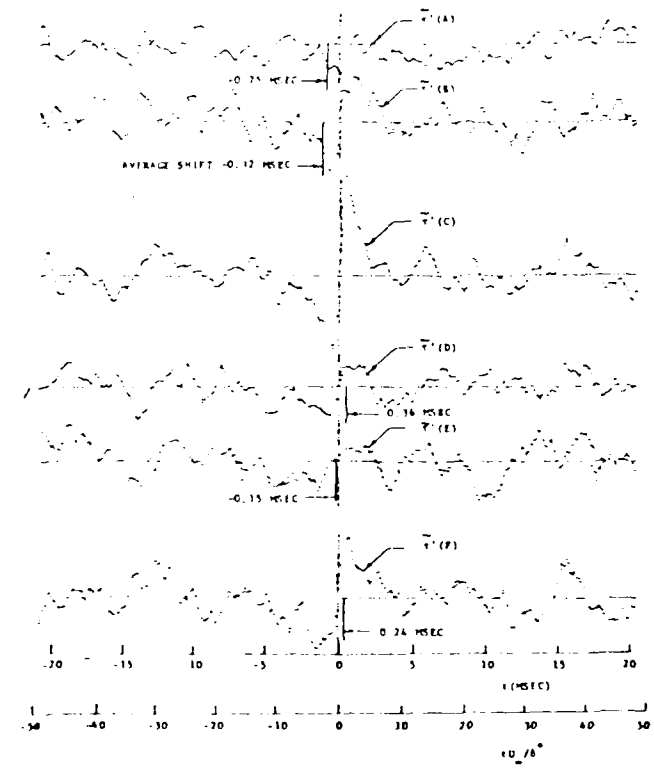

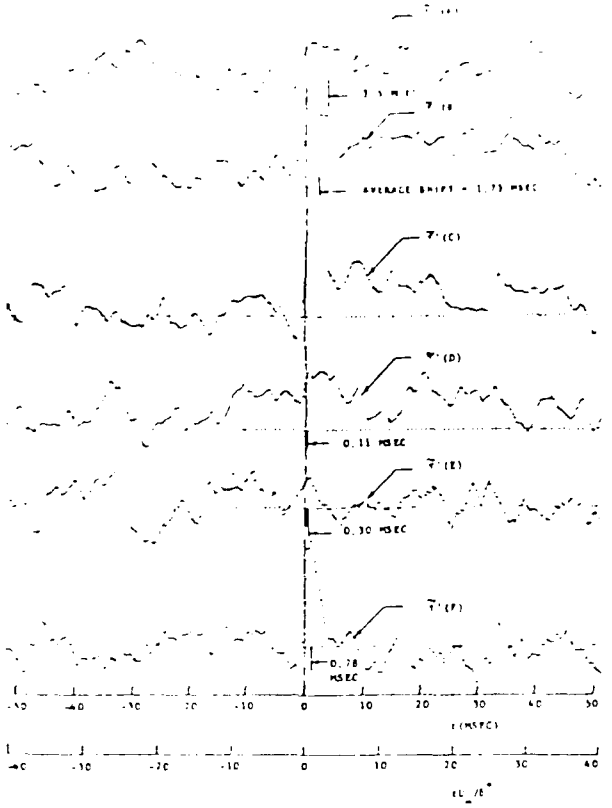

Fig 20 Ensemble averaged wall shear fluctuations for the array of Figure 2 after correction for phase "jitter" (only events with positive shifts between $\tau'(C)$ and $\tau'(B)$)
U_∞ = 32.6 ft/sec, trigger: $\tau'(C)$

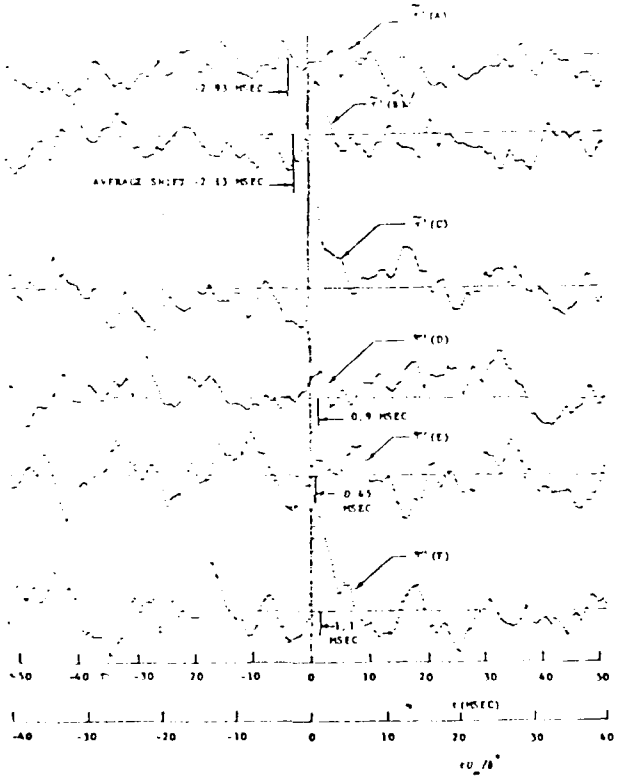

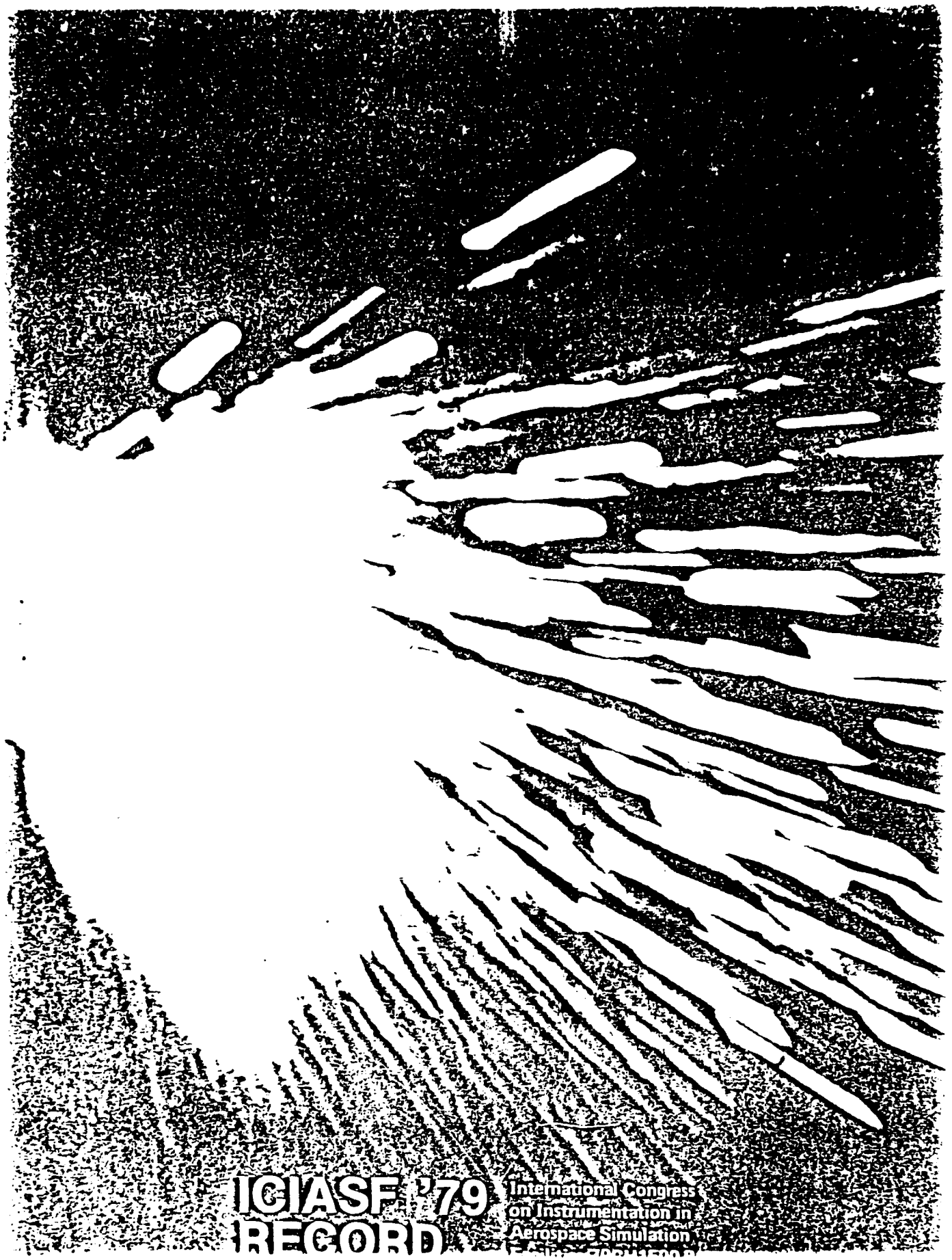

ICIASF '79 RECORD

International Congress on Instrumentation in Aerospace Simulation

MEASUREMENTS OF THE COHERENT STRUCTURE OF BOUNDARY LAYER TURBULENCE AT A HIGH SUBSONIC SPEED

V. Barra and K. Hozumi

New York University - Antonio Ferri Laboratories

Westbury, N.Y.

Abstract

The instrumentation and data analysis procedures utilized to study the organized nature of boundary layer turbulence are described. Measurements in the boundary layer consist of the streamwise velocity and wall-shear using miniature hot-film sensors and constant temperature anemometers, and wall-pressure using piezoresistive transducers and low-noise differential amplifiers. Procedures for recording, digitizing, and analyzing the fluctuating components of these measurements with the aid of a mini-computer system are outlined. The digital analyses performed include conventional Fourier transform and time-averaged correlation, as well as conditional sampling to obtain ensemble averaged time signatures and correlations of the fluctuations for coherent events in the flow. Representative results obtained from these analyses for three free stream conditions are presented.

1. INTRODUCTION

The discovery, by means of visual observations (Refs. 1-7), of an organized structure in turbulent shear flows has led to a proliferation of new measurement and data analysis procedures for the investigation of the fluctuating peoperties of such flows (Refs. 8-19). Questions have been raised concerning the adequacy of measurements which utilize instrumentation and analyses not suited to the multi-scale, quasi-periodic nature of the flow structures that have been observed. It has been found that the size of the transducers used in the measurements and the frequency response of the associated electronics is an important consideration in terms of the varied scales of the flow structures; and that single point measurements and conventional time averaged analyses cannot reveal much useful information about coherence or intermittency, both of which are important aspects of the flow processes involved.

To overcome these problems, modern research efforts have turned to minituarized instrumentation and multiple measurements to obtain some sort of spatial resolution of the coherent flow structures, and to digitization of the measurements so as to allow various time series analyses to be performed on high speed computers. With respect to the latter, it has become increasingly popular to apply various conditional sampling procedures to the digitized fluctuations in order to isolate temporal sequences associated with the coherent structures. This type of analysis has revealed, among other things, that significant contributi to the long time average Reynolds stress occur during intervals when coherent structures are present in the flow, thus indicating that the modelling of turbulence and the development of d and noise reduction mechanisms might benefit greatly from a better understanding of these structures.

Visual observations of turbulent boundary layer flows seeded with various tracers have indicated the presence of several different processes involving repetitive flow structures. Th wall region ($y^+ < 100$) is characterized by strea wise streaks of low speed fluid which lift up fr the wall resulting in locally inflexional veloci profiles. The lift-up is followed by some sort oscillatory motion and then a sudden breakup int small scale turbulence. The ejection of low spe fluid from the wall is accompanied by sweeps of high speed fluid from the outer regions toward t wall. This overall process has been referred to a "burst" (Refs. 20-21). On a larger scale, the boundary layer is dominated by vortical structur which extend to the viscid-inviscid region (Refs 14, 16). The relationship or interaction betwee this large-scale outer structure (LSOS) and the turbulent "bursts" is still not clearly defined. In particular, how these processes and their relationship change with increasing Reynolds numb has not been fully explored. On the basis of observations and measurements over a limited range Reynolds numbers, it has become commonly accepte that the "bursting" process is strictly a sublaye phenomenon that scales with wall variables, while the large-scale outer structure is basically Reynolds number independent. A possible link between the two processes may exist in the fact that the frequency of occurrence of the turbulen "bursts" has been found to scale with outer flow variables and seems to be related to the period o passage of the outer structures (Refs. 22-23).

The primary objective of the present investi gation has been to obtain information concerning these phenomena at high subsonic speeds, and to specifically determine the possible role or influence of pressure fluctuations on the processes involved. The experiments discussed here were therefore performed in a boundary layer with a relatively high (compared to other investigations in this area) free stream velocity (U_∞ = 675 ft/s and Reynolds number ($Re_\theta \approx 10^5$). In addition, an instrumentation and data acquisition system was developed that allows simultaneous measurements t

be made of three properties of the turbulent flow, namely, the streamwise velocity, the wall-shear and the wall-pressure. Up to twelve such measurements have been analyzed digitally on a mini-computer using procedures similar to those developed to study these phenomena in low speed flows (Refs. 8, 14, 24, and 25). For the purpose of comparison, the measurements and analyses have also been performed for free stream velocities of 75 and 32.6 ft/sec.

2. INSTRUMENTATION AND DATA RECORDING

The measurements described here were made on or near the wall of a 12 inch diameter induction wind tunnel, a sketch of which is shown in Fig. 1. The details of the construction and calibration of this facility can be found in Refs. 19 and 26. The original design of the tunnel included a sonic throat section which allowed the speed in the test section to be varied from M = 0.6 to 0.8. Modifications were made to the throat section centerbody that now allow the speed to be set as low as 30 ft/sec. Arrangements were also made to allow the test section to be placed at various distances from the inlet depending on the boundary layer thickness required for the measurements.

The types of sensors used for the measurements and the general method of placement in the tunnel are sketched in Fig. 2. The test section is fitted with four windows, two of which can be used to mount the plug containing the wall-shear and wall-pressure sensors and the rake of five streamwise velocity probes. A sixth velocity measurement is made very near the wall with a special subminiature probe mounted directly in the tunnel window. The electronics associated with recording the fluctuating output signal of each sensor are shown in Fig. 3. The mean and rms levels of the signals are monitored during tests either visually on meters or on a chart recorder. The specifics of the instrumentation for each type of measurement are as follows:

a) Wall-Pressure

The wall-pressure is measured using flush-mounted Kulite type MIC-080-5 piezoresistive transducers which are rated for a pressure difference of 5 psi. The pressure sensitive area of these transducers has a diameter of 0.040" (see Fig. 2). The sensitivity of each transducer was checked and found to be constant up to the rated pressure and to be on the order of 0.6 mV/psi/V(input). With a bridge excitation of 9 volts, a dynamic calibration of these transducers using a pistonphone yielded an equivalent sensitivity of 142 dB below 1.0V/μbar. The manufacturer specified natural frequency of 200 kHz insures that this sensitivity is accurate up to approximately 40 kHz.

The output signal from these transducers is conditioned by Princeton Applied Research type 113 low-noise amplifiers. Because of the high gain required (typically on the order of 2000), the amplifiers were operated in a differential mode so as to alleviate the problem of induced electronic noise. (Proper shielding and grounding were also found to be helpful in this regard). Filtering provided for on the amplifiers by a set of low a high frequency, 6dB/octave, roll-off filters. T typical bandpass used was 10-100,000 Hz, althoug it was sometimes necessary to lower the upper er to 30,000 Hz to help eliminate high frequency no

b) Wall-Shear

A Thermo-Systems type 1237 flush-mounted ho film sensor together with a DISA 55A01 constant temperature anemometer are used to measure the shear on the wall beneath the boundary layer. T wall-shear is determined from the bridge output voltage according to the well established relati ship (see, for example, Thomas (Ref. 15)):

$$E_b^2 = A\,\tau_w^{1/3} + B$$

The applicability of this relationship in the present case will be discussed in a subsequent section.

The dynamic characteristics of the sensor depend on how the coefficients A and B in the a relation vary with frequency and on the time response characteristics of the anemometer feedbac circuit. The later was adjusted using the stand square wave calibration procedure to give a flat response curve up to approximately 20 kHz. The range of frequencies for which the relationship between the output voltage and wall-shear remain unchanged will depend on the hot-film dimensions and substrate material and on the flow conditio as discussed by Thomas (Ref. 15). For the case U_∞ = 675 ft/sec, these considerations lead to frequency limits of

$$190\ \text{Hz} < f < 21\ \text{kHz}$$

which should not be of serious consequence in t of the frequencies of interest in the present measurements.

c) Streamwise Velocity

The streamwise velocity in the boundary lay is measured with Thermo-Systems type 1260 and 12 hot-film probes and various types of constant temperature anemometer systems (Fig. 3). The sensing element on these probes is an alumina coated cylindrical quartz rod having a diameter 0.001" and a lateral width of 0.040" for the 126 type probes and 0.010" for the single 1297 subminiature probe. Calibration of the five probes the rake is accomplished in a small induction tunnel built specifically for this purpose. The flow speed in the tunnel can be varied continuo from zero to approximately 600 ft/sec and can be kept steady for long periods of time. The flow speed is determined from the ratio of static to stagnation pressure as measured with a precise s of manometers. The bridge output voltage-veloci relationship obtained from the calibration is us to set-up the analog linearizers shown in Fig. 3 or to linearize the data representing the stream wise velocity after it has been digitized.

The frequency response of these systems is checked using a square wave calibration signal and adjusted to give a flat response up to about 20 kHz although some variation existed from one system to another. The bandpass on the signal conditioners was typically set at 5-50,000 Hz.

Recording of the analog fluctuation signals from these various sensors is provided for by a Honeywell 5600 tape recorder which has 13 available data channels. To achieve the most suitable data bandwidth, recording is done in FM mode at a speed of 60 IPS. In this configuration the available bandwidth is DC-40 kHz. Two signals which serve to synchronize the different data channels on playback are recorded along with the sensor signals during each test. One is a pulse train with a period of about 1.5 seconds which serves to separate the test into several sections. The other is a 200 kHz sine wave which acts as a tape-time clock in the digitizing procedure. Since only 13 data channels are available on the tape recorder, the pulse train had to be added to one of the sensor signals when 12 measurements were made in the flow.

3. DATA ACQUISITION AND ANALYSIS SYSTEMS

The recorded data is analyzed with the systems shown schematically in Fig. 4. Conventional spectral and correlation analyses of the analog data are performed using a General Radio 1900 wave analyzer and a Saicor 42 correlation and probability analyzer. The bulk of the data analysis, however, is performed on digitized sections of the recordings obtained with the use of a PDP-11/34 minicomputer system. This system includes the 11/34 processor with 64K bytes of memory, one RL01 cartridge disk drive and dual floppy disk drives for mass storage, two terminals-one of which has a CRT with graphics and hard-copy capability, and, most significantly for the present application, a 64 channel A/D converter with two programmable clocks. The software available on the system includes the RT-11 operating system, a Fortran IV compiler, and several scientific subroutine and laboratory applications packages.

Several considerations led to the development of the digitizing procedure being used in this experiment. The requirement that fluctuation frequencies as high as 40 kHz be accurately resolved (particularly for the wall-pressure) implied the need for sampling rates on the order of 100 kHz or preferably 200 kHz. To achieve such a high sampling rate and still maintain the simultaneity of 12 data channels would require, even with the procedure of slowing down the tape recorder on playback, a very specialized A/D system with multiple sample-and-hold circuits and fast settling and conversion times. With the procedure described here, an effective sampling rate of 200 kHz/channel can be easily achieved for any number of channels even with the relatively inexpensive and limited A/D system available on the mini-computer (i.e., the AD11K). One of the limitations of this system is that it has a single sample-and-hold circuit, thereby making it impossible to achieve strict simultaneity when sampling more than one channel under normal procedures. The requirement that the measurements be simultaneous is very important in terms of the analyses to be performed on the data.

The procedure used to achieve these requirements involves digitizing a single data channel at a time in order to relax the need for very high overall sampling rates, and employing the recorded 200 kHz sine wave to determine when samples are to be taken thereby preserving the simultaneity of the group of channels digitized. The data is played back at 1/64 the speed at which it was recorded (i.e., 15/16 IPS) starting at a point just before one of the pulses on the pulse train channel (indicated as 1 in Fig. 4). Sampling begins on the occurrence of this pulse and is repeated at each occurrence of an appropriate signal on the External A/D-Start input of the A/D system. This is provided by a pulse generator driven by the 200 kHz (3.12 kHz in real-time) sine wave on the recorder (indicated as 2 in Fig. 4). Due to the limited memory available, a maximum of approximately 10,000 samples can be made with one pass through the conversion program. This data is written on disk and the process repeated for each data channel on the recorder.

It can be seen that the sine wave becomes a clock (for time on the tape) having a resolution of 5 μsec. As such it can be used to precisely locate information on the tape. For example, if more than 10,000 samples are required the clock can be used to measure a 10,000 interval delay between the occurrence of the pulse and the start of the next set of 10,000 samples. This process can be repeated almost indefinitely if the sine wave is sufficiently free of noise so that timing errors do not accumulate. It is also possible in the conversion program to make the timing interval any integer multiple of the basic 5 μsec, thus allowing the data to be sampled at any rate that is an integer fraction of 200 kHz.

As with the digitizing procedure, the required analyses of the data had to be adapted to the constraints of the 11/34 system. The problem of the limited memory available was overcome through the use of overlays in the analyses programs and by analyzing the long data records (typically 30,000 points) in blocks of 512 points at a time. To minimize data access time in this procedure, the RL01 disk drive is used as the primary or direct mass storage device. The slow speed of the 11/34 processor is an unavoidable disadvantage of the system, the solution of which would be to transfer the digitized data to a faster machine. The possibility of doing this with a CDC-6600 is being investigated.

The analyses that can now be performed on a production run basis on the 11/34 include the following:

- Long time average auto and cross correlations
- Conditional sampling of the data using the variable interval time average (VITA) variance to isolate temporal sequences associated with

coherent events in the flow (see Kaplan and Laufer (Ref. 24) or Blackwelder and Kaplan (Ref. 8)). Ensemble averages can be formed from a set of events.

- Pattern recognition analysis to compensate for random phase "jitter" in conditional samples (see Blackwelder (Ref. 25))

- Short-time, conditionally sampled auto and cross correlations (see Brown and Thomas (Ref. 14)).

These analyses can be applied to the original data or to the data after it has been filtered using a Fast Fourier Transform (FFT) algorithm to include only fluctuation components in a chosen frequency range. In addition an attempt has been made to see what benefits could be gained by incorporating certain aspects of one type of analysis into another.

4. MEASUREMENTS

The mean flow parameters at several stations in the tunnel for the three flow conditions for which measurements have been made are summarized in Table I. Details on the measurement of the mean velocity and turbulent intensity profiles can be found in Refs. 19 and 26. It should be noted that the boundary layer thickness is on the order of 4" in all cases, while the Reynolds number ranges from approximately 5,000 to 100,000.

Once the mean properties of the flows were determined, simultaneous measurements were made of the fluctuations in the flow with the sensor array shown in Fig. 2. A more detailed lay-out of this array is presented in Fig. 5. The six hot-film velocity measurements (I,J,K,L,O,M) are made within a distance of approximately 1/2" from the tunnel wall. The hot-film at y = .025"(M) is the type 1279 subminiature probe described previously. A table of the various non-dimensional distances from the wall for the different flow conditions is also included in Fig. 5. The measurement of the wall-shear with the flush mounted hot-film sensor (F) is made directly below the velocity measurements. Five of the Kulite pressure transducers (T,S,R,Q,P) are aligned in the streamwise direction directly upstream of the wall-shear sensor. The spacing of the measurements was determined strictly on the basis of placing the sensors as close as physically possible. The primary effort of the present experiment has been directed toward measurements with this array, although more recently efforts have also been made to set-up and make measurements with a lateral array of sensors.

The first analysis performed on the measurements with this array was to obtain the spectral distributions of the fluctuations. This was done directly from the recorded analog data. An early conclusion reached from this analysis was that the levels of the wall-pressure fluctuations for the two low-speed cases were much higher than expected. As a result of many previous measurements it is to be expected that the rms level of the wall-pressure fluctuations will fall somewhere between 0.5% and 1% of the dynamic pressure, q_∞. In the case of U_∞ = 675 ft/sec we measured a reasonable level of 0.008 q_∞. But at U_∞ = 73 ft/sec and 32.6 ft/sec the measured levels were equivalent to approximately 0.23 q_∞ and 0.65 q_∞, respectively. The explanation for this is that, for the low speed tests, the wall-pressure fluctuations due to the turbulent boundary layer become so weak that they drop below the noise "floor" of the measuring devices. The noise "floor" is made up primarily of tunnel noise, although other sources such as transducer vibration response and misallignment with the tunnel wall may also contribute to it.

It is thought that the level of tunnel noise could be lowered with extensive acoustic treatment of the sonic throat section of the tunnel (where the flow undergoes rapid acceleration) and by improving the suspension system of the tunnel. Besides the time involved, several factors influenced the decision not to undertake these modifications. First, in the high subsonic regime, where primary interest lies, the wall-pressure fluctuations due to the turbulent boundary layer are thought to be sufficiently above the noise "floor" to allow for accurate measurements. Secondly, in the low speed cases the main interest is in looking at the wall-shear and fluctuation velocity profiles (for comparison to those obtained at high speed), the measurement of which should not be significantly affected by tunnel noise. And lastly, the measurement of very low pressure levels would require much more sensitive transducers than are now being used.

Typical power spectra obtained for the wall-pressure fluctuations are shown in Fig. 6. Those measured by Serafini (Ref. 27) and Wooldridge and Willmarth (Ref. 28) are also shown for comparison. It can clearly be seen that for the two low speed flows the noise "floor" is anywhere from 20 to 40 dB above the expected wall-pressure fluctuations over the entire range of pertinent frequencies. In the high speed case the measured fluctuations have a spectral distribution which agrees more favorably with previous measurements. The lower levels obtained above $u\delta^*/U_\infty \approx .3$ could be due to the size of the transducer not allowing accurate resolution of small-scale fluctuations.

A comparison of previous measurements seems to indicate that if the transducer diameter is too large, a loss of resolution of small-scale pressure fluctuations will occur. This manifests itself as consistently lower measured spectral densities at high frequencies, that is, above $u\delta^*/U_\infty \approx 1$. Emmerling (Ref. 11) has summarized the available results in terms of the non-dimensional parameter du_τ/ν, where d is the transducer diameter. For values of this parameter above approximately 100 the overall rms level of the wall-pressure fluctuations is always measured to be around $0.005q_\infty$. Below this value, the measured rms level increases linearly as du_τ/ν is lowered. This increase is attributed to the increased resolution of intense small-scale fluctuations, or equivalently of high frequency spectral components, by the smaller

transducers. (More recent results seem to indicate that a good part of this increase can be attributed to errors introduced by the use of pinhole microphones (see Ref. 29)). For the transducer used here, $du_\tau/\nu \approx 300$ (for $U_\infty = 675$ ft/sec) thus indicating that some loss of resolution probably exists in the present measurements. The reasons for the high overall level of 0.008 q_∞ have not been determined.

An additional question concerning sensor size arises for the flush mounted hot-film sensor. It has been found (see Thomas (Ref. 15)) that the bridge output voltage-wall shear relationship given in Section 2 holds only if

$$7.8 < \frac{L_e u_\tau}{\nu} < 46$$

where L_e is the effective length of the sensor in the streamwise direction. For a sensor width, W, of about twice the length, Thomas finds that $L_e/L_a \approx 2.6$. Using this ratio in the present case ($L_a = 0.005$") would yield an $L_e u_\tau/\nu$ of about 100, 20 and 12 for $U_\infty = 675$, 73 and 32.6 ft/sec, respectively. But since W/L_a is larger than 2 (i.e., ≈ 8), the ratio L_e/L_a will also be smaller than 2.6, thereby giving a more acceptable value of $L_e u_\tau/\nu$ for $U_\infty = 675$ ft/sec.

Power spectra for the velocity fluctuations at two points in the boundary layer are presented, together with similar data obtained by Wooldridge and Willmarth (Ref. 29), in Figs. 7,8 and 9 for the three free-stream velocities. In all three cases there is reasonable agreement in the overall shape and level of the spectral distributions. This confirms the assumption that unlike the wall-pressure fluctuations, the velocity fluctuation measurements are not significantly affected by tunnel noise in the lower speed flows. The differences in the spectra at the two measurement positions, particularly for $U_\infty = 675$ ft/sec (Fig. 7), is most likely due to the difficulty in matching the frequency response characteristics of the different anemometers used for the measurements. It should be noted that for the velocity fluctuation spectra, the local mean velocity and not the free-stream velocity has been used to non-dimensionalize frequency.

Representative of the type of results obtained from conditional sampling of the digitized data are the ensemble averages shown in Figs. 10a and b and the sequence of fluctuation and total velocity profiles shown in Figs. 11 and 12. These results are for $U_\infty = 675$ ft/sec and were obtained by applying the VITA variance analysis to the velocity fluctuations at y = .075"(0) to detect the occurrence of flow processes with certain repetitive characteristics. An ensemble average is then taken of a short interval of data centered about these detection points for each of the measurements in the flow. The results, presented in Figs. 10a and b, show that the flow structures triggering the detection scheme are, on the average, highly coherent over the entire set of measurements. These flow structures are obviously some aspect of the large scale outer structure since the detector is located in the outer region (i.e., $y^+ = 568$). The high degree of correlat of the wall measurements to the passage of the outer structures may be due to the fact that t wall sensors, due to their size, are biased to the large scales associated with the outer structures. The typical sensor dimension of 0. represents approximately 300 viscous lengths a $U_\infty = 675$ ft/sec, thereby making it impossible resolve wall region processes such as "bursts" which are thought to have lateral scales on th order of 50 ν/u_τ. Irregardless of this argume however, it would seem that the strong and dir influence of the outer structure on the fluctu at the wall in this high speed flow may have practical importance and should be studied fur

From the ensemble averages shown in Fig. it is possible to depict the behavior of the i stantaneous fluctuation (Fig. 11) and total (F velocity profiles during the passage of the av flow structure. The similarities between the sequence of profiles shown in Figs. 11 and 12 those obtained by Blackwelder and Kaplan (Ref. in the wall region of a low speed (14 ft/sec) have been noted in Ref. 19. The ensemble aver obtained in the present investigation for the speed flows ($U_\infty = 73$ and 32.6 ft/sec) seem to indicate that these similarities can be accoun for in one of two ways. Either, as has also b suggested by Chen and Blackwelder (Ref. 16), t wall region "bursts" display the same type of signatures in terms of the streamwise velocity certain aspects of the large scale outer struc or the detection scheme being used in all thes cases triggers on some "typical" structure whi can be found in various regions of the boundar layer.

Without going into great detail, some of other analyses performed on the data are as follows:

- In the ensemble averages it is sometimes necessary, particularly when the separation between the detector and the measurement being averaged is large, to compensate for random variations in the arrival times of events at the two positions. This is done by a pattern recognition analysis which corrects for this phase "jitter" (see Blackwelder (Ref. 25)). Without this procedure it is possible for any coherence that exists to be lost in the noise that results from the randomness in phase.

  Long-time average cross correlations have been used to infer information concerning overall convection velocities and spatial representations of the turbulence. By looking at short-time correlations over conditionally sampled sections of data, this type of information can also be obtained for particular flow structures.

- Filtering of the data in all the analyses discussed thus far using the FFT can be useful in determining the importance or influence of different frequency ranges on particular results. By correlating the low frequency part of a measurement with some representation of the high frequency components some information could be obtained concerning the relationship between the large scale structures and small scale phenomena such as "bursts" (see Brown and Thomas (Ref. 14)). This would be particularly applicable to the wall measurements.

Future plans include the expansion of a lateral array of sensors for which some measurements have already been made. These measurements have thus far only involved wall-shear sensors in an attempt to obtain some information concerning the lateral geometry of the flow structures. It is planned that this array will be expanded to include wall-pressure and streamwise velocity measurements aligned in the lateral direction. To accomplish this it will be necessary to expand the number of anemometer channels available. This is being done by the construction of as many as 20 simple anemometer sets similar in principle to the circuit discussed by Weidman and Browand (Ref. 30), and also to one developed by R.E. Kaplan at U.S.C. The use of these anemometer sets will greatly simplify calibration and frequency matching procedures, but will require additional processing, e.g., linearizing, of the digitized data.

5. CONCLUSIONS

A facility has been established for studying the coherent structure of boundary layer turbulence at high subsonic speeds. This includes an induction wind tunnel with a 12" diameter test section, an instrumentation package for measuring the velocity, wall-shear and wall-pressure in the boundary layer developed on the wall of the tunnel, and a data analysis system capable of digitizing the measurements and performing relevant conditional processing of the data.

Although primary interest lies in the high subsonic regime ($U_\infty \approx 700$ ft/sec), measurements can and have been made in turbulent boundary layers with free stream velocities as low as 30 ft/sec. The boundary layer thickness is typically between 3 to 4", although again the wind tunnel has the flexibility to allow measurements to be made at various positions in the development of the flow. The instrumentation package gathered for the measurements includeshot-film velocity probes, flush mounted hot-film wall-shear sensors and flush mounted piezoresistive wall-pressure transducers. Calibration procedures have been established for the velocity probes and pressure transducers while a standard output voltage-shear relationship is used to reduce the signal from the wall-shear sensors. The instrumentation and associated signal conditioning and recording electronics allow for bandwidths of up to 20 kHz for the velocity and shear fluctuations and 40 kHz for the pressure fluctuations.

Data analysis equipment is available for performing standard spectral and correlation analyses of the analog data and a specialized digitization procedure has been developed to produce discrete time sequences of the fluctuations. With this procedure, sampling rates as high as 200 kHz/channel can be achieved while maintaining the simultaneity of 12 recorded data channels. This is accomplished using a relatively unsophisticated A/D conversion system that is part of a PDP-11/34 laboratory mini-computer system.

All the analysis of the digitized data is performed on this mini-computer system. This includes the use of a short-time average variance technique to locate the occurience of coherent events in the data and then forming ensemble averages of these events. A pattern recognition analysis can be performed to improve the ensemble averages by compensating for random variations in the arrival time of the events at different points in the flow. A different approach to conditional sampling involving short-time cross-correlations can also be applied to the data. In addition, all these analyses can be performed after appropriate filtering of the data using a Fast Fourier Transform subroutine.

Measurements have been made for three free stream velocities (i.e., U_∞ = 675, 73, 32.6 ft/sec) with an array of sensors which attempts to resolve the velocity profile at a station normal to the wall, the wall-shear directly below, and the wall-pressure in the streamwise direction directly upstream. Typical spectra of the fluctuations agree favorably with previous measurements except for the wall-pressure in the two low speed flows. In these cases the pressure fluctuations due to the turbulent boundary layer appear to be well below a noise "floor" which is thought to be made up primarily of tunnel noise. In the high speed flow a problem exists with the resolution of the very small-scale phenomena associated with the wall layer by the relatively large pressure and shear sensors. The benefits that could be gained in this regard by using a commercially available transducer with a sensitive area having a diameter 0.010" will be investigated.

The application of the conditional sampling analyses to the measurements has led to several interesting results particularly in the high speed case where investigations of this type are scarce. The analysis of this data is continuing while plans are being made to expand the total number of measurements in the grid and to set-up a lateral array of measurements to obtain information about the flow structures in this direction.

REFERENCES

1. Kline, S.J., Reynolds, W.C., Schraub, F.A., and Runstadler, P.W., "The Structure of Turbulence," Journal of Fluid Mechanics, 30:741, 1967.

2. Corrino, E.R. and Brodkey, R.S., "A Visual Investigation of the Wall Region in Turbulent Flow," Journal of Fluid Mechanics, 37:1, 1969.

3. Kim, H.T., Kline, S.J., and Reynolds, W.C., "The Production of Turbulence Near A Smooth Wall in a Turbulent Boundary Layer," Journal of Fluid Mechanics, 50:113, 1971.

4. Offen, G.R. and Kline, S.J., "Combined Dye Streak and Hydrogen Bubble Visual Observations of a Turbulent Boundary Layer," Journal of Fluid Mechanics, 62:223, 1974.

5. Falco, R.E., "Some Comments on Turbulent Boundary Layer Structure Inferred from the Movements of a Passice Contaminant," AIAA Paper No. 74-99, 1974.

6. Falco, R.E., "Coherent Motions in the Outer Region of Turbulent Boundary Layer," Physics of Fluids, 20:S124, 1977.

7. Smith, C.A., "Visualization of Turbulent Boundary Layer Structure Using a Moving Hydrogen Bubble-Wire Probe," Proc. of the Work shop on Coherent Structure of Turbulent Boundary Layers, p. 48, 1978.

8. Blackwelder, R.F. and Kaplan, R.E., "The Intermittent Structure of the Wall Region of the Turbulent Boundary Layer," U. Southern California, A.E. Report No. 1-22, 1972.

9. Wallace, J.M., Eckelman, H., and Brodkey, R.A., "The Wall Region in Turbulent Shear Flow," Journal of Fluid Mechanics, 54-39, 1972.

10. Lu, S.S. and Willmarth, W.W., "Measurements of the Structure of the Reynolds Stress in a Turbulent Boundary Layer," Journal of Fluid Mechanics, 60:481, 1973.

11. Emmerling, R., "The Instantaneous Structure of The Wall Pressure Under a Turbulent Boundary Layer," Max-Planch-Institut fur Stromungschung Rep. No. 9, 1973.

12. Dinkelacker, A., Hessel, M., Meier, G.E.A., and Scheve, G., "Investigation of Pressure Fluctuations Beneath a Turbulent Boundary Layer by Means of an Optical Method," Physics of Fluids, 20:S216, 1977.

13. Zilberman, M., Wyganski, I., and Kaplan, R., "Transitional Boundary Layer Spot in a Fully Turbulent Environment," Physics of Fluids, 20:S258, 1977.

14. Brown, G.L. and Thomas, A.S.W., "Large Structure in a Turbulent Boundary Layer," Physics of Fluids, 20:243, 1977.

15. Thomas, A.S.W., "Organized Structure in the Turbulent Boundary Layer," Lockheed-Georgia Report LG77ER0210, 1977.

16. Chen, C.P. and Blackwelder, R.F., "Large-scale Motion in a Turbulent Boundary Layer: A Study Using Temperature Contamination," Journal of Fluid Mechanics, 89:1, 1978.

17. Eckelman, H., Wallace, J.M., and Brodkey, R.A., "Pattern Recognition, a Means for Detection of Coherent Structures in Bounded Turbulent Shear Flows," Proc. of the Dynamic Flow Conference, p. 161, 1978.

18. Wygnanski, I., "The Recognition of an Evoked Large-Scale Structure in Turbulent Shear Flows," Proc. of the Dynamic Flow Conference, p. 191, 1978.

19. Zakkay, V., Barra, V., and Wang, C.R., "The Nature of Boundary Layer Turbulence at a High Subsonic Speed," AIAA Journal, 17:356, 1978.

20. Offen, G.R. and Kline, S.J., "A Proposed Model of the Bursting Process in Turbulent Boundary Layers," Journal of Fluid Mechanics, 70:209, 1975.

21. Kline, S.J., "The Role of Visualization in the Study of the Structure of the Turbulent Boundary Layer," Proc. of the Workshop on Coherent Structure of Turbulent Boundary Layers, p. 1, 1978.

22. Rao, K.N., Narasimha, R., and Badri Narayanon, M.A., "The Bursting Phenomenon in a Turbulent Boundary Layer," Journal of Fluid Mechanics, 48:339, 1971.

23. Laufer, J. and Bardi Narayanan, M.A., "Mean Period of the Production Mechanism in a Boundary Layer," Physics of Fluids, 14:182, 1971.

24. Kaplan, R.E. and Laufer, J., "The Intermittently Turbulent Region of the Boundary Layer," 12th Proc. Int. Congr. Mech., p. 236, 1969.

25. Blackwelder, R.F., "On the Role of Phase Information in Conditional Sampling," Phys. Fluids, 20:S232, 1977.

26. Zakkay, V., Barra, V., and Hozumi, K., "Investigation of the Fluctuation Mechanism in Turbulent Flow," Final Report prepared under Contract AFOSR-76-2497, December 1978.

27. Serafini, J.S., "Wall-Pressure Fluctuations and Pressure Velocity Correlations in Turbulent Boundary Layers," AGARD Report 454, 1963.

28. Wooldridge, C.E. and Willmarth, W.W., "Measurements of the Correlation Between the Fluctuating Velocities and the Fluctuating Wall Pressure in a Thick Turbulent Boundary Layer," U. of Michigan Report 02920-2-T, 1962.

29. Willmarth, W.W. and Bogar, T.J., "Survey and New Measurements of Turbulence Structure Near the Wall," Physics of Fluids, 20:S9, 1977.

30. Weidman, P.D. and Browand, F.K., "Analysis of a Simple Circuit for Constant Temperature Anemometry," Journal of Physics E: Scientific Instruments, 8:553, 1975.

x/D	13.2	20.3	9	13.5	31	51
$\bar{u}/U_\infty$	0.0763	0.0798	0.063	0.067	0.072	.86
U_∞ (ft/sec)	39.6	32.6	69.0	73.0	78.0	675
q_∞ (psi)	0.0060	0.0086	0.059	0.066	0.076	2.9
δ (in)	2.7	3.5	2.15	3.0	~ 5.5	6.0
δ^* (in)	0.39	0.497	0.265	0.51	~ 0.9	0.584
θ (in)	0.31	0.387	0.206	0.29	~ 0.6	0.384
Re_θ	4.67×10^3	6.56×10^3	8.43×10^3	1.75×10^4	2.82×10^4	1.08×10^5
$\sqrt{\bar{u}^2}/U_\infty$ (in)	1.66×10^{-3}	1.09×10^{-3}	$.69 \times 10^{-3}$	$.67 \times 10^{-3}$	$.68 \times 10^{-3}$	1.32×10^{-4}
$\sqrt{\bar{u}^2}/U_\infty$ (wall)	320	53.6	26.0	22.5	23.0	0.67
$\overline{uv}/U_\infty^2$	0.003	-	-	0.005	0.021	0.008

TABLE 1 MEAN FLOW PARAMETERS AT SEVERAL STATIONS FOR THREE TEST CONDITIONS

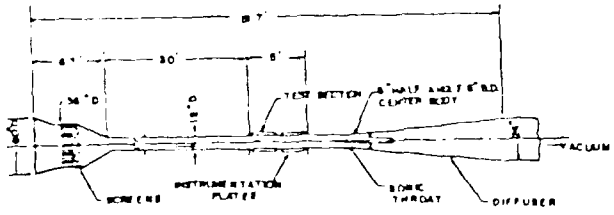

FIG. 1 WIND TUNNEL

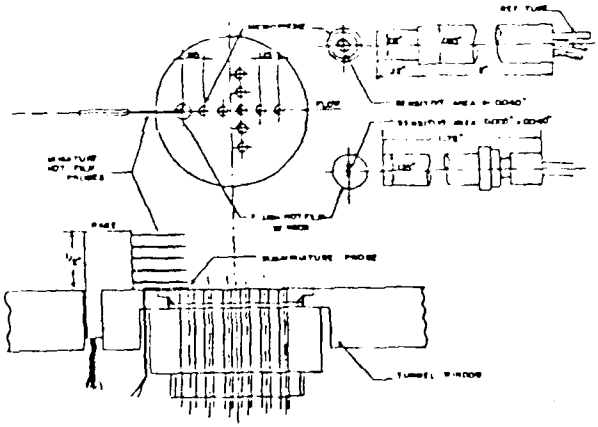

FIG. 2 DETAILS OF INSTRUMENTATION SET-UP

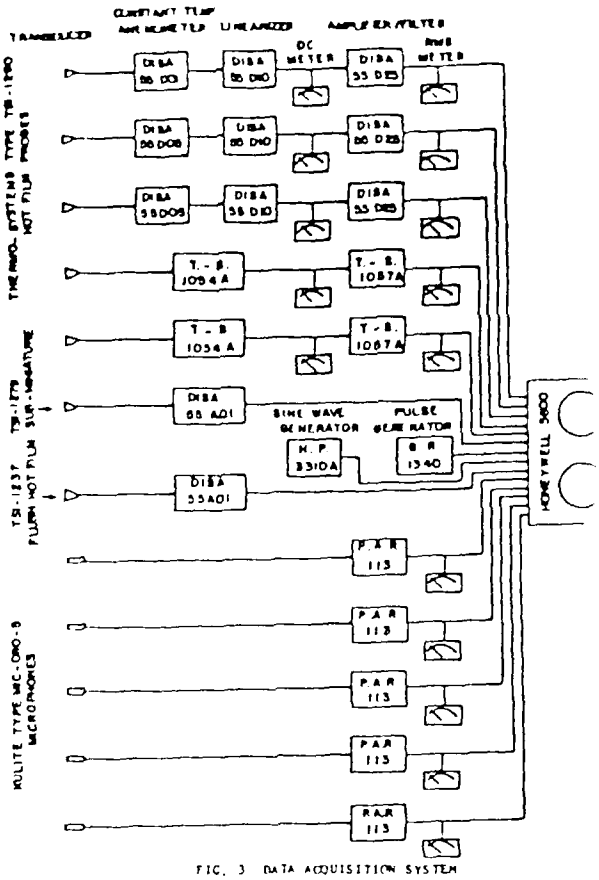

FIG. 3 DATA ACQUISITION SYSTEM

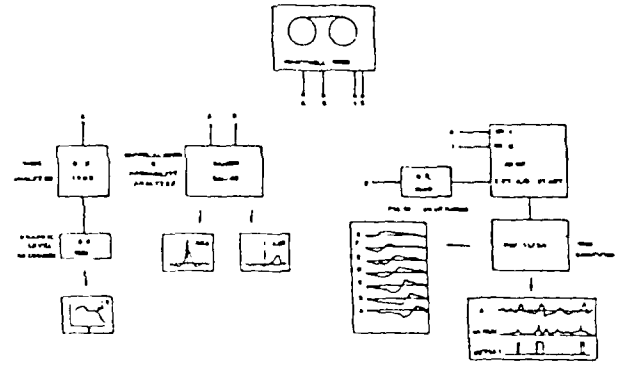

FIG. 4 DATA ANALYSIS SYSTEMS

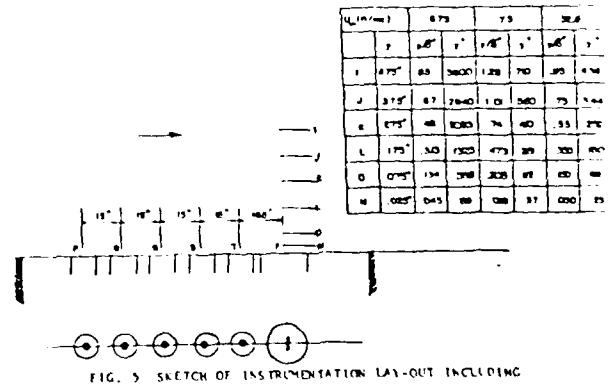

FIG. 5 SKETCH OF INSTRUMENTATION LAY-OUT INCLUDING TABLE OF NON-DIMENSIONAL DISTANCES FROM WALL

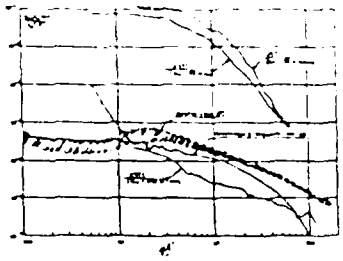

FIG. 6 TYPICAL SPECTRA OF THE WALL-PRESSURE FLUCTUATIONS

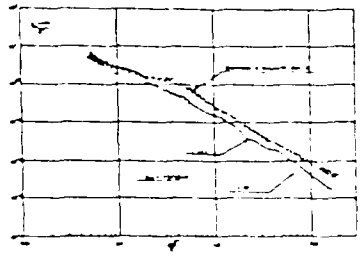

FIG. 8 TYPICAL SPECTRA OF THE VELOCITY FLUCTUATIONS FOR U_∞ = 73 FT/SEC

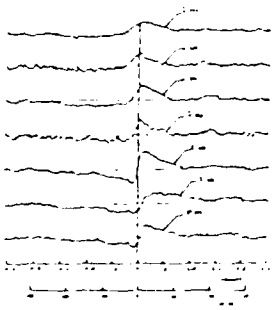

FIG. 10a ENSEMBLE AVERAGED VELOCITY AND WALL-SHEAR FLUCTUATIONS
U_∞ = 675 FT/SEC, TRIGGER: u'(0)

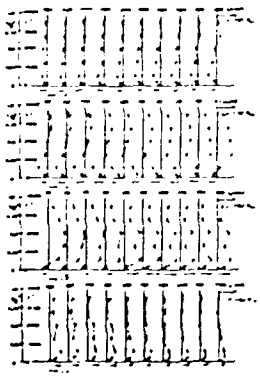

FIG. 11 SEQUENCE OF VELOCITY FLUCTUATION PROFILES AND FLUCTUATING SHEAR OBTAINED FROM THE ENSEMBLE AVERAGES IN FIG. 10a (U_∞ = 675 FT/SEC)

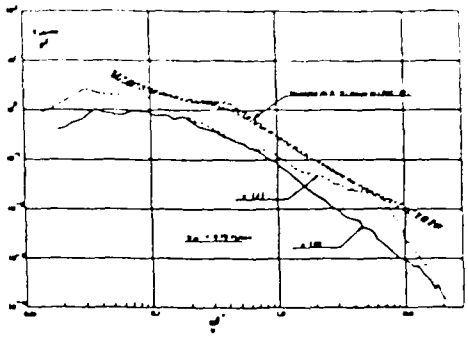

FIG. 7 TYPICAL SPECTRA OF THE VELOCITY FLUCTUATIONS FOR U_∞ = A

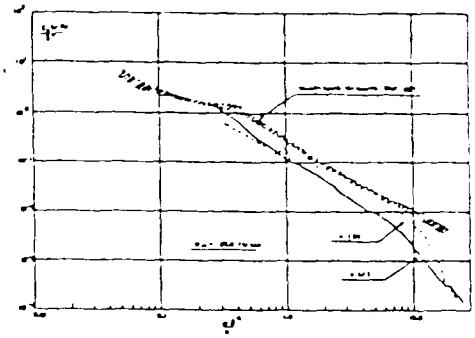

FIG. 9 TYPICAL SPECTRA OF THE VELOCITY FLUCTUATIONS FOR U_∞ = 12

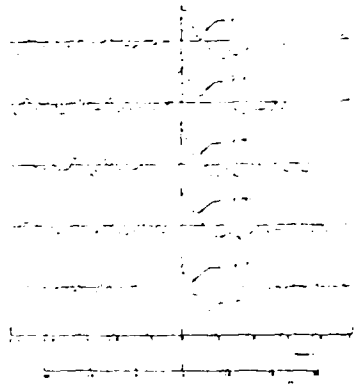

FIG. 10b ENSEMBLE AVERAGED WALL-PRESSURE FLUCTUATIONS
U_∞ = 675 FT/SEC, TRIGGER: u'(0)

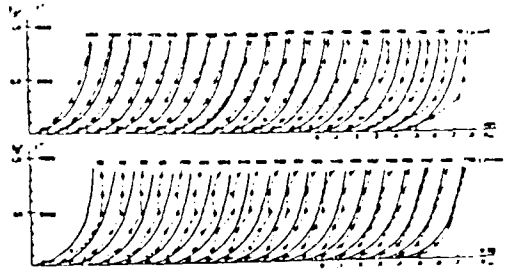

FIG. 12 SEQUENCE OF TOTAL VELOCITY PROFILES OBTAINED FROM THE ENSEMBLE AVERAGES IN FIG. 10a (U_∞ = 675 FT/SEC)